ARMY RESEARCH LABORATORY

Examining the Feasibility of a Method of Tripwire Detection Using Acoustics

by Kevin Sanchez and W. C. Kirkpatrick Alberts, II

ARL-TN-0379 **December 2009**

NOTICES

Disclaimers

Army Research Laboratory
Adelphi, MD 20783-1197

ARL-TN-0379 **December 2009**

Examining the Feasibility of a Method of Tripwire Detection Using Acoustics

Kevin Sanchez and W. C. Kirkpatrick Alberts, II
Computational and Information Sciences Directorate, ARL

REPORT DOCUMENTATION PAGE	*Form Approved* *OMB No. 0704-0188*

1. REPORT DATE *(DD-MM-YYYY)* December 2009

2. REPORT TYPE

3. DATES COVERED (From - To)

4. TITLE AND SUBTITLE
Examining the Feasibility of a Method of Tripwire Detection Using Acoustics

5a. CONTRACT NUMBER

5b. GRANT NUMBER

5c. PROGRAM ELEMENT NUMBER

6. AUTHOR(S)
Kevin Sanchez and W. C. Kirkpatrick Alberts, II

5d. PROJECT NUMBER

5e. TASK NUMBER

5f. WORK UNIT NUMBER

7. PERFORMING ORGANIZATION NAME(S) AND ADDRESS(ES)
U.S. Army Research Laboratory
ATTN: RDRL-CIE-S
2800 Powder Mill Road
Adelphi, MD 20783-1197

8. PERFORMING ORGANIZATION REPORT NUMBER
ARL-TN-0379

9. SPONSORING/MONITORING AGENCY NAME(S) AND ADDRESS(ES)

10. SPONSOR/MONITOR'S ACRONYM(S)

11. SPONSOR/MONITOR'S REPORT NUMBER(S)

12. DISTRIBUTION/AVAILABILITY STATEMENT
Approved for public release; distribution unlimited.

13. SUPPLEMENTARY NOTES

14. ABSTRACT
A major objective in developing tools and weapons for military use has always been ensuring the safety of Soldiers and actively making them aware of hazards in their environment. One such hazard is tripwires hidden in the field. Current research investigates a method of detecting trip wires using an air flow aimed at a wire to generate sound that can then be detected using a microphone. The work presented here examines the effect of varying tension, distance, nozzle type, and air flow rate on the generated sound. Should this technique prove viable, the equipment's size would permit usage on small robots. This technique when coupled with other sensors in a multi-modality approach could increase the probability of detection of tripwires.

15. SUBJECT TERMS
Acoustic tripwire detection

16. SECURITY CLASSIFICATION OF:			17. LIMITATION OF ABSTRACT	18. NUMBER OF PAGES	19a. NAME OF RESPONSIBLE PERSON
a. REPORT	b. ABSTRACT	c. THIS PAGE			Kevin Sanchez
Unclassified	Unclassified	Unclassified	UU	54	19b. TELEPHONE NUMBER (*Include area code*) (301) 394-5649

Standard Form 298 (Rev. 8/98)
Prescribed by ANSI Std. Z39.18

Contents

List of Figures

List of Tables

INTENTIONALLY LEFT BLANK.

1. Introduction

The U.S. Army Research Laboratory is developing a class of robots to reduce the casualty risk of military and civilians by detecting hazards they could come across in their environment (*1*). One potential task for a robot is the detection and identification of trip wires.

Technologies exist to detect trip wires by using video imaging tools on the robots and applying them to locate a fine line, which would indicate the presence of a trip wire. One problem with this method of detection is difficulty in differentiating between a trip wire and the edge of a rigid object, such as the corner of a table (*1*). The second problem is that trip wires are meant to be hidden, which makes the use of imaging tools less promising.

Another option considered to detect trip wires was the use of lasers. Lasers can be used to scan a 2D area and record its position and the time delay of the scattered signal to determine the distance and dimensions of an object (*1*). The setback with this form of detection is that lasers can have trouble accurately detecting a wire due to its small cross-sectional area (*1*).

This report investigates the feasibility of detecting trip wires by using a controlled flow of air across a wire to detect the broadband noise generated (*2*). The solid object, a wire in this case, will create broadband noise that is created by the eddies in the air. When air is forced out of a nozzle it has a velocity and the moving air spreads out, pushes and mixes with the surrounding air until it becomes stable (*3, 4*). When the air flows, small eddies are created because of the difference in air speed between the flowing air and the still laboratory air. When these eddies collide with an object, such as a wire, more turbulence is created and there is a detectable increase in sound level. There is no exact way to setting up a trip wire in a trap. Usually any type of thin wire could be used for the job and it may be tight or very loose and free to swing (*5*). Almost anything can be used from fishing line to phone cords. Therefore, for this technique of trip-wire detection to be reliable, detecting all of these possible situations such as loose and tight wires is important along with a large variety of possible trip wires that may be used.

In the following section the experimental configuration is discussed. The next section contains the results of the experiment and presents an analysis of said results. The last section explains future points of revision on how to proceed with the experiment.

2. Experiment

In the experiment, four wires (see table 1) were tested along with 4 different types of nozzles (see figure 1 and table 2). Each nozzle and each wire was used with 6 different air flow rates from 10–60 standard cubic feet per hour (scfh) in increments of 10 scfh ± 2 scfh. Testing a wire at different flow rates allowed them to be compared to see what rate worked best or if certain flow rates were better for particular wires. The air that flows from a given nozzle creates a relatively constant background noise and air flow pattern unique from the other nozzles. Therefore, different nozzle backgrounds were recorded with the microphone. The microphone was placed at a constant 3 cm directly above the nozzle and oriented at 90°, 45°, and 0° relative to the plane of the nozzle (see figure 2). Each combination of wire, nozzle and pressure was used at six, 1-cm increments between the wire and nozzle. This enabled the ability to test how far the wire could be from the microphone and nozzle before only the nozzle's background noise was detected. These tests were also run having the wires at different tensions, 0.5, 1.0, and 1.5 kg with a digital spring scale with an uncertainty of ±10 g to determine how the signal changes under different amounts of tension.

Table 1. Wires tested.

Tripwire Simulant	**Diameter (mm)**
1 conductor speaker wire	2.93
White cotton string	~2.0
Non-insulated mild steel wire	0.64
Round nylon fishing line	0.25

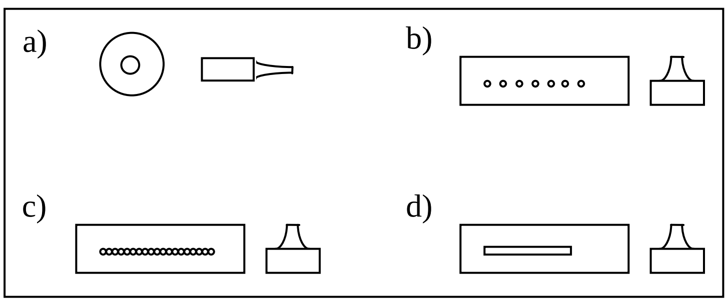

Figure 1. (a) Single-hole nozzle, (b) 7-hole nozzle, (c) 19-hole nozzle and (d) Slit nozzle.

Table 2. Nozzles tested.

Nozzles	**Distance between Holes (mm)**	**Diameter of Holes (mm)**
Single-hole	N/A	2.438
7-hole	7.62	1.422
19-hole	2.54	0.964
Slit Nozzle	Length (mm)	Width (mm)
Slit	15.24	0.794

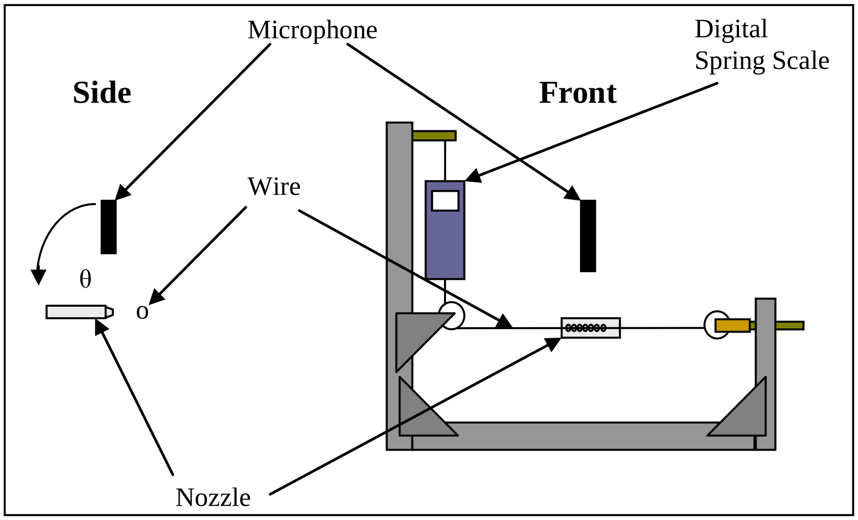

Figure 2. Experiment configuration.

The noise spectra were collected using an Ono-sokki multi-purpose FFTAnalyzer CF-5210 filtered with a 20 kHz Butterworth lowpass filter. The frequency range of the data was 0–20 kHz and 30 averages were taken for each run. The microphone was a B&K 4192 half-inch condenser microphone.

3. Results and Discussion

For this technique to be feasible, the broadband noise from the wire needed to be loud enough for the microphone to detect it over the nozzle and ambient background and at a reasonable distance. Figure 3 shows the ambient background of the lab and figure 4 shows the background noise of each nozzle when there is no wire in front of it. Figure 5, which plots wire noise spectra normalized by the nozzle spectrum, shows that a 5 dB increase of noise above the nozzle noise was able to be detected 5 cm away from the wire from 0–20 kHz.

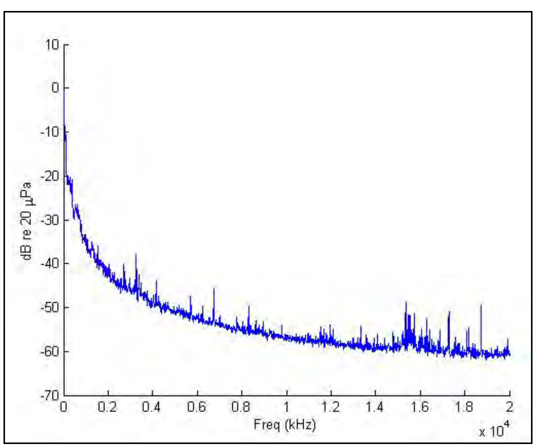

Figure 3. Noise spectrum of ambient background in lab.

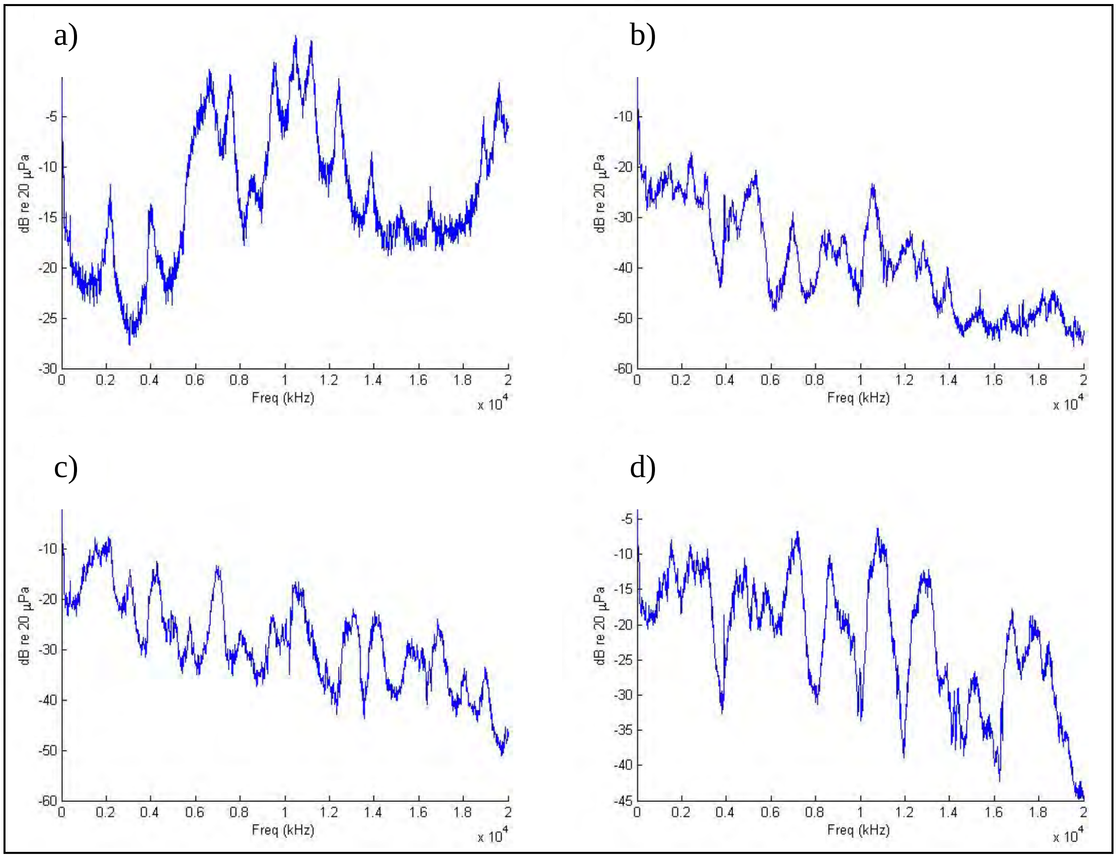

Figure 4. Noise spectra for each nozzle at 30 scfh. (a) Single-hole nozzle, (b) 7-hole nozzle, (c) 19-hole nozzle, and (d) Slit nozzle.

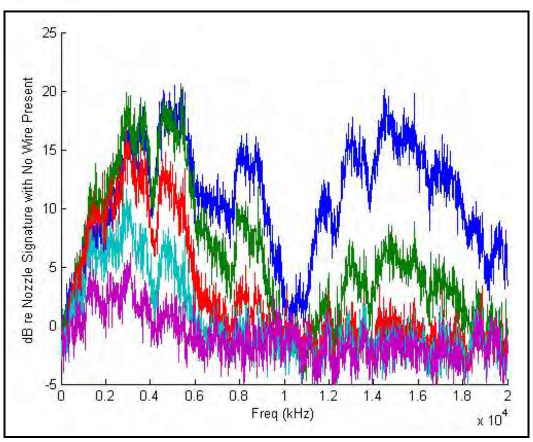

Figure 5. Noise spectra showing: one conductor speaker wire with 1.5 kg tension; using single-hole nozzle at 60 scfh; microphone at 0°. A blue curve represents a nozzle-wire separation of 1 cm, green-2 cm, red-3 cm, teal-4 cm, and purple-5 cm.

Unfortunately, figure 5 is not representative of most of the data collected. Most results contained little to no differences in background noise further than 2–3 cm. The nozzles played a large part in altering our results because they affect how the air hits the wire and how concentrated or spread out the flow of air is. The nozzles themselves also created a great deal of background noise, which overwhelmed the signal from the wire and caused the wire to not be detected (*6*).

The four nozzles were tested with the goal of finding which nozzle provided the best results to optimize the distance the nozzle could be from the wire and still have the microphone be able to detect the signal. There was also the possibility to consider that certain nozzles may be better at generating noise when paired with certain wires so each wire was tested with each nozzle. Figure 6 is an example of how the nozzle with the single-hole provided much better results than the other nozzles. The other nozzles created too much background noise, which masked any noise generated by flow over the wire. See appendix A. Some wires and other air flow rates did produce better data though, overall, the single-hole nozzle created better results for all the wires.

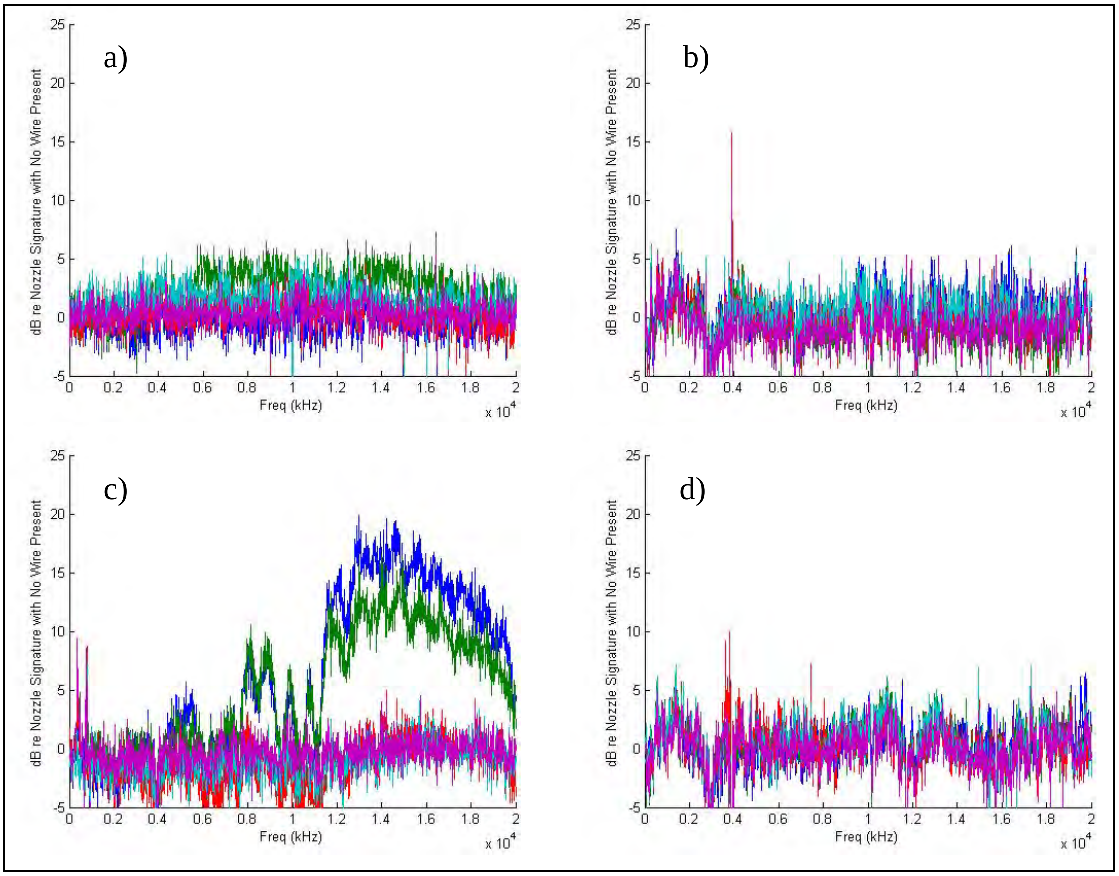

Figure 6. Noise spectra showing the effects of different nozzles: fishing line with zero tension; 10 scfh; microphone at 90°. (a) 7-hole nozzle, (b) 19-hole nozzle, (c) single-hole nozzle, and (d) nozzle with slit. Color representation as in figure 5.

The air flow rate affected our data in that higher air flows caused more background noise from the nozzle. A larger air flow also meant that the speed of the air as it came into contact with the wire would be different. The larger air flow should have created a louder sound when it hit the wire. The air flow did create differences in the results, which were related to the diameter of the wire and type of nozzle used. The nozzle used determined which air flow rates gave optimal results. Also, the diameter of the wire was related to how much a different flow rate affected the outcome. For example, in figure 7 the single-hole nozzle was used and the optimum air flow rate was about 10 scfh. As is evident in figure 7c, the increase to 30 scfh, using fishing line as the wire, greatly affected the results in that there was a dramatic decrease in the signal detected. Larger wires produced significant broadband noise. Another relation appeared to be between the amounts of background noise a nozzle created and the optimal flow rate to produce detectable noise. The relationship between them was unclear but the optimal flow rate was not consistently the same for each nozzle.

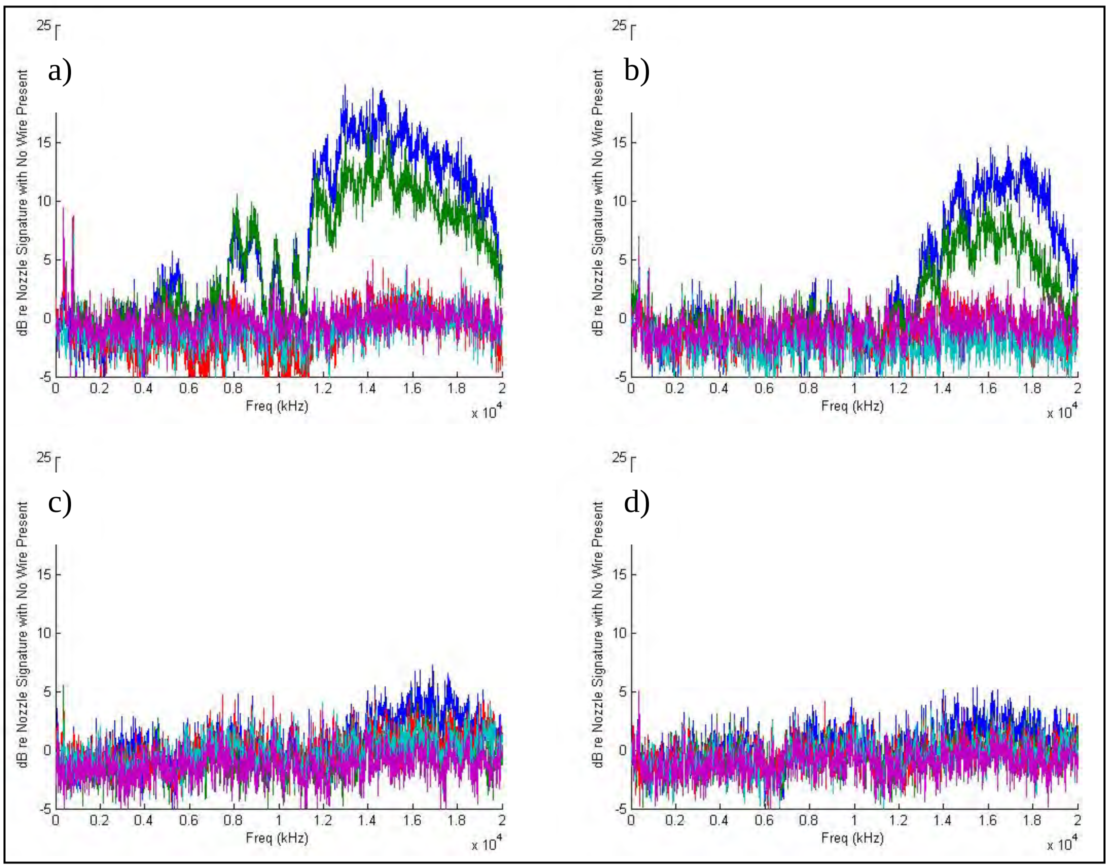

Figure 7. Noise spectra showing the effects of different air flow rates: fishing line with zero tension; using single-hole nozzle; microphone at 90°. (a) 10 scfh, (b) 20 scfh, (c) 30 scfh, and (d) 40 scfh. Color representation as in figure 5.

The noise generated by each wire was unique under each set of circumstances, but each wire's spectrum retained its structure when the air flow rate was changed. Wires with larger diameters were easier to detect than wires with smaller diameters. As is shown in figure 8, the noise spectrum depends on the diameter of the wire. The plots for each wire are shown from smallest to largest in figure 8 from a to d. Trends shown in figure 8 were common throughout the experiments. It was also apparent that the largest increases in level due to the wire's diameter occur at low frequency, below 10 kHz.

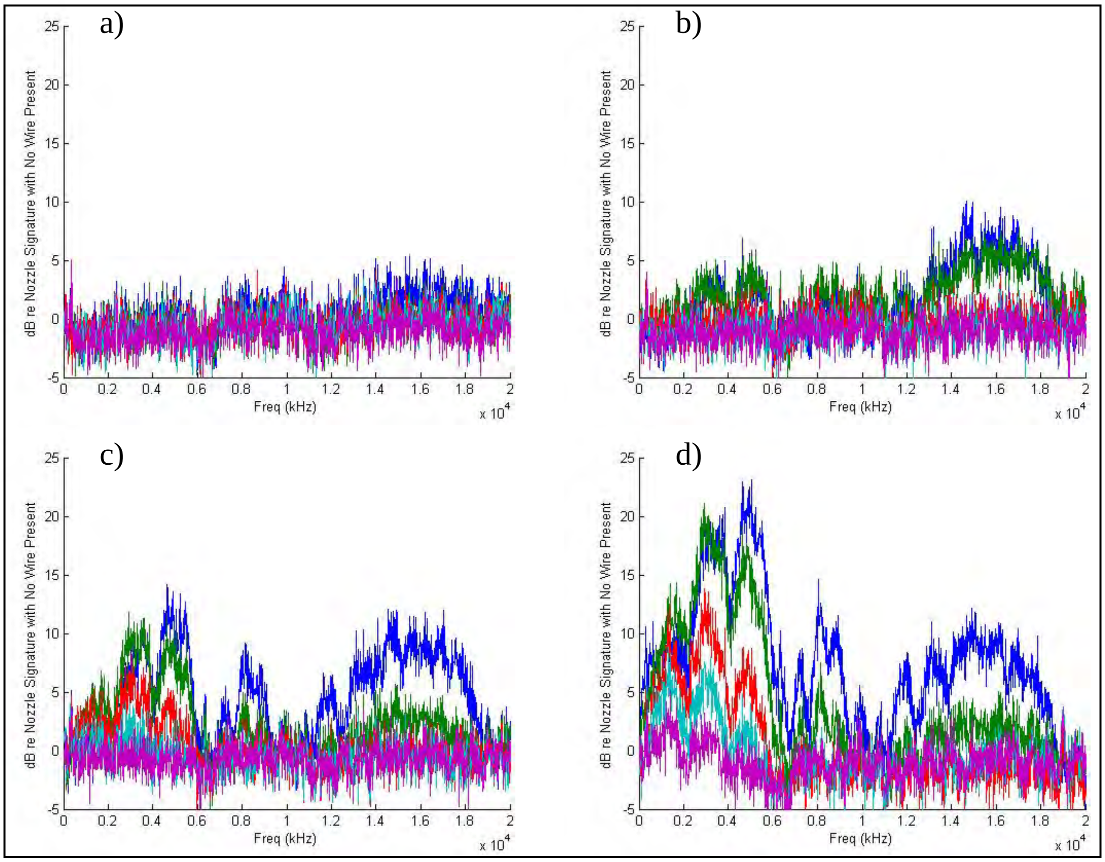

Figure 8. Noise spectra showing the effects of different wires: zero tension; single-hole nozzle at 40 scfh; microphone at 90°. (a) Round nylon fishing line, (b) non-insulated mild steel wire, (c) white cotton string, and (d) 1 conductor speaker wire. Color representation as in figure 5.

Trip wires are likely not consistently tied at one specific tension, so it was important that different tensions were tested. The wire tension made little difference in any of the results. Only when no tension was on the wire, as shown in figure 9a, did there seem to be a slight drop in dB. In figure 9 the spectrum is shown with the wire at 4 different tensions. This pattern was also consistent with all of the other wires that were tested, showing that tension is not a limiting factor on this technique's ability to detect a wire. See appendix B.

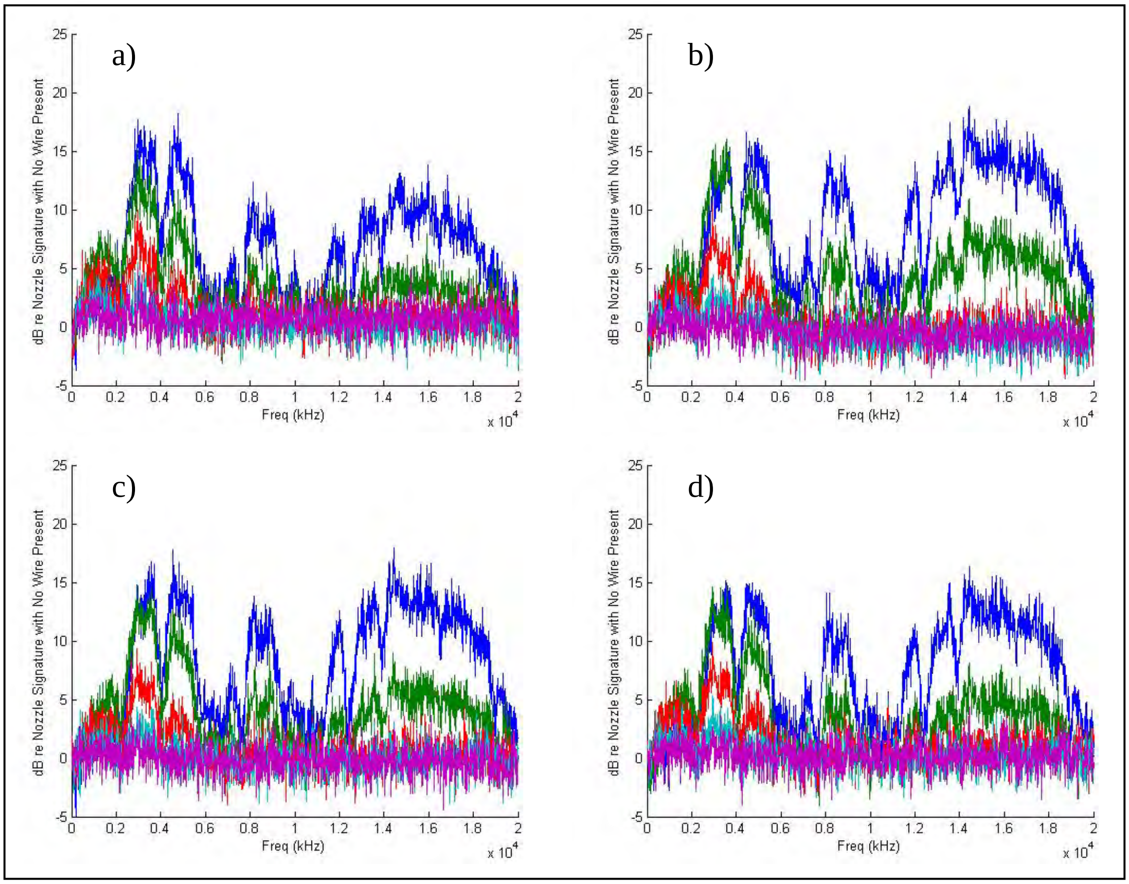

Figure 9. Noise spectra showing the effects of different tensions: white cotton string; using single-hole nozzle at 30 scfh; microphone at 0°. (a) zero tension, (b) .5 kg tension, (c) 1.0 kg tension, and (d) 1.5 kg tension. Color representation as in figure 5.

In an attempt to extend the distance a wire could be detected, the microphone was shifted to different angles. At different angles the microphone might detect less of the nozzle noise, while detecting more of the signal coming from the wire. As the angle of the microphone changed, the level of the wire's noise spectrum changed; it decreased when the microphone was pointed 90°. In figure 10 it is evident that at 0° and 45° the signal was slightly larger and could be detected better at larger distances. See appendix C.

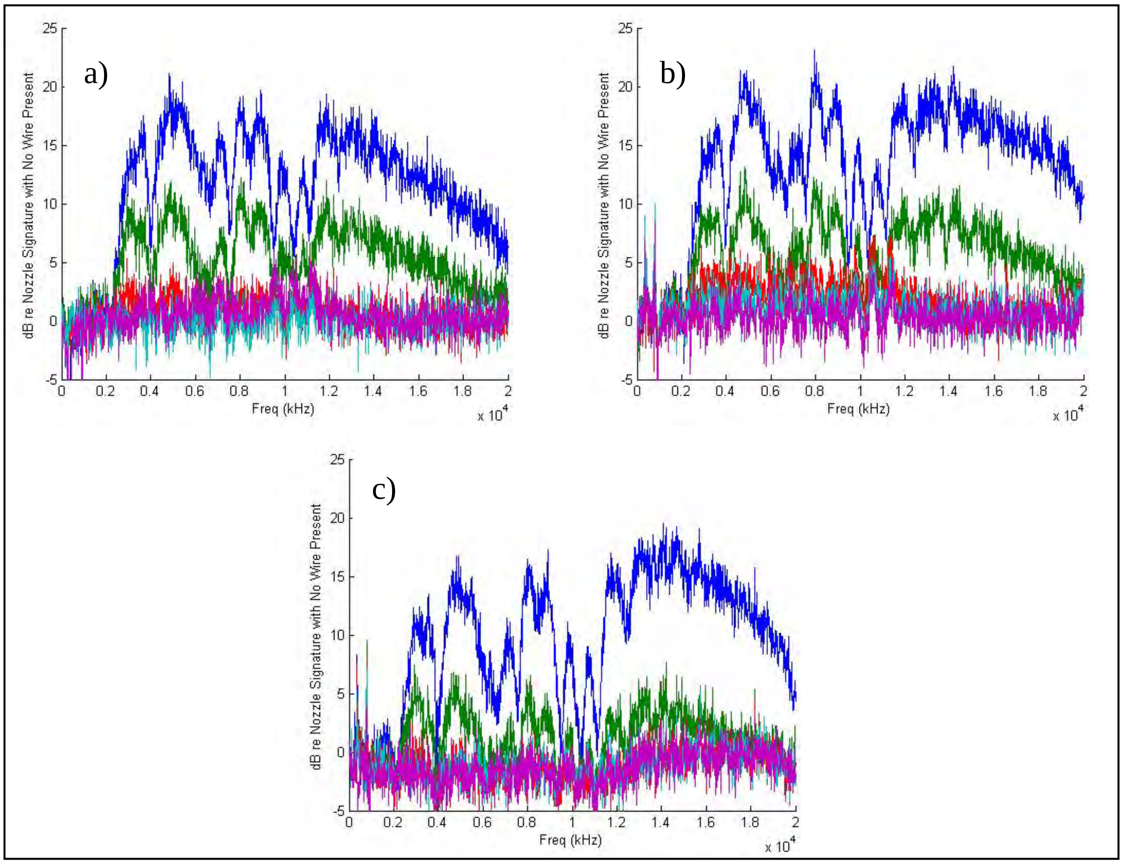

Figure 10. Noise spectra showing the effects of different microphone angles: non-insulated mild steel wire with zero tension; using single nozzle at 10 scfh. (a) microphone at 0°, (b) microphone at 45°, and (c) microphone at 90°. Color representation as in figure 5.

It may be useful to couple this technique with another method. For instance, video imaging techniques mentioned in the introduction, have trouble distinguishing between what could be a wire or a straight edge of an object such as a table. The method described here could be used as a confirmation to probe the spot where a line appeared on the video image. If the line is a wire, signals similar to those depicted in figures 5–10 will appear for a short period of time as the system probes the area by moving the nozzle up and down parallel to the wire. If the line is a corner, then increased noise will be detected for a long period of time indicating the line could be a corner or edge like in figure 11.

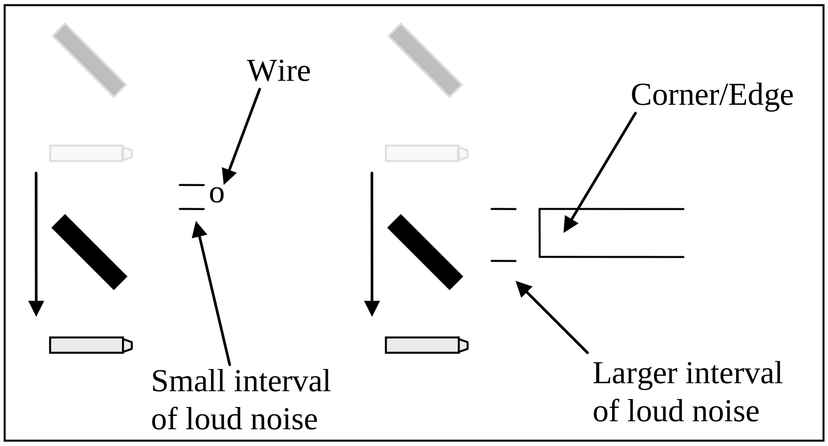

Figure 11. Motion of microphone and nozzle used to probe an area to detect the presence of a wire or corner.

4. Summary and Conclusions

Results have shown that the single-hole nozzle, which was quietest, worked best. Flow rates do alter the level of the signal, but no one rate had shown to consistently be better for all the wires. This method does not rely on tension, eliminating the concern on detectability for different tensions. For this to become implemented though, much more information is needed. However, based on the results presented here, this method of detecting trip wires using acoustics is feasible.

Theoretical calculations need to be performed to find why certain things improved the detection ability to further determine how to enhance this technique. Also, an effective way to analyze the information received by the microphones needs to be developed that helps the user decide if there is a wire present or not. More patterns are unknown such as how exactly air flow rate and wire type affect each other. Overall the technique does work and now more in-depth work needs to be done in order to realize the full potential of this technique.

5. References

1. Young, S.; Budulas, P.; Emmerman, P.; Scanlon, M.; Srour, N.; Hillis, D.; Fisher, P.; Vinci, S.; Harrison, A.; Gurton, K.; Crow, S.; Wellman, M. *RRSTA for Small Rover in Urban Warfare*; ARL-TR-1678; U.S. Army Research Laboratory: Adelphi, MD, 11–12, May1999.

2. Zaitsev, M. Y.; Kopiev, V. F. Mechanism of Sound Rradiation by Turbulence Near a Rigid Body. *Fluid Dynamics* **2008**, *43*, 86–96.

3. Davis, M.; Pan, N. Noise Generated by the Interaction of Turbulent Jets with Circular Cylinders. *J. Sound Vib.* **1989**, *135* (3), 427–442.

4. Powell, A. Nature of the Sound Sources in Low-speed Jet Impingement. *J. Acoust. Soc Am.* **1991**, *90* (6), 3326–3331.

5. Carter, L. J.; Liao, L.C.Y. An Optimal Technology for Detection of Vegetation-obscured Tripwires. *Proc. SPIE* **2006**, *6217*, J2172–J2172.

6. Moore, P.; Slot, H.; Boersma, B. J. Simulation and Measurement of Flow Generated Noise. *J. Comp. Phys.* **2007**, *224*, 449–463.

INTENTIONALLY LEFT BLANK.

Appendix A. Each Wire and Nozzle Combination

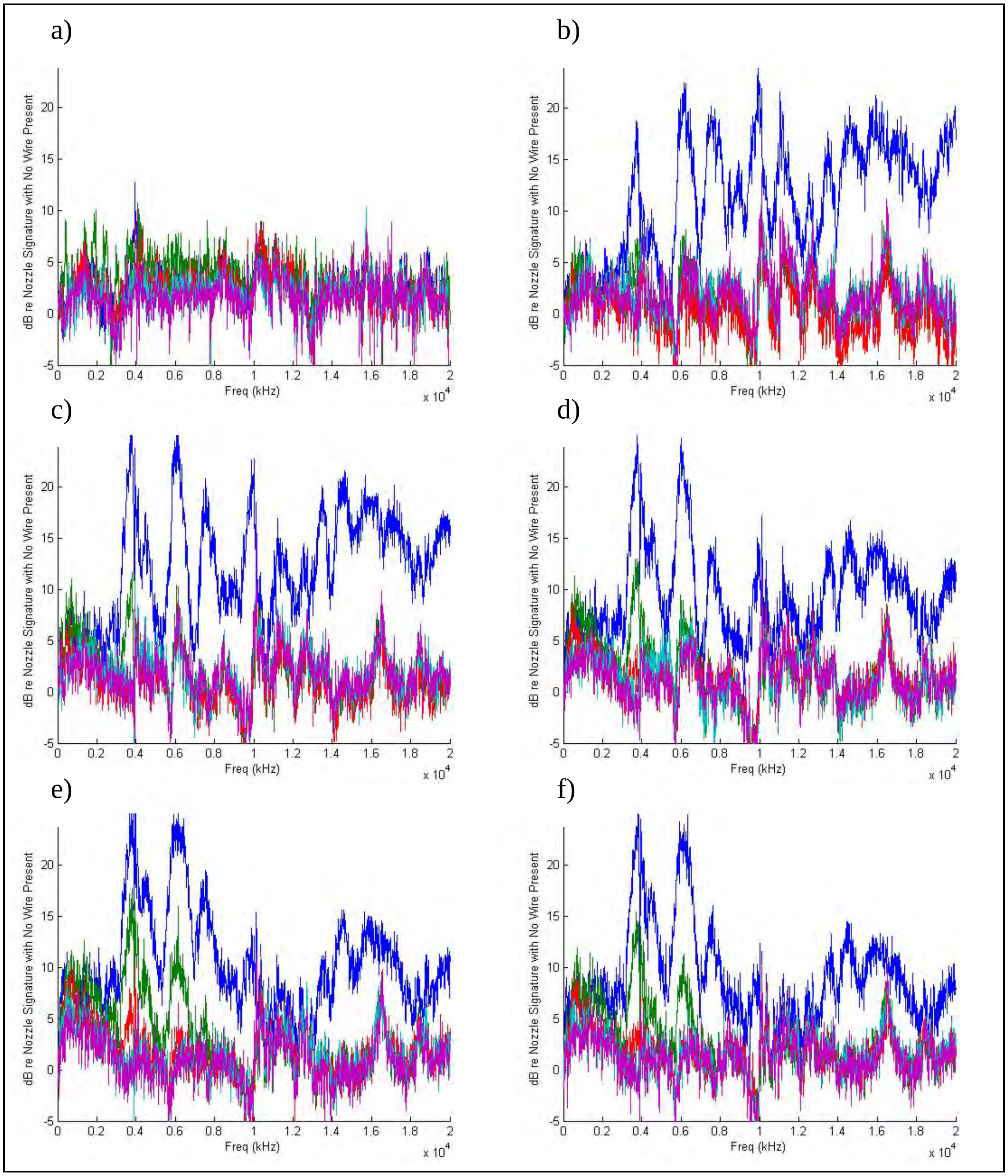

Figure A-1. 7-hole nozzle with 1 conductor speaker wire, zero tension, microphone at 90° (a) 10 scfh, (b) 20 scfh, (c) 30 scfh, (d) 40 scfh, (e) 50 scfh, and (f) 60 scfh. Color representation as in figure 5.

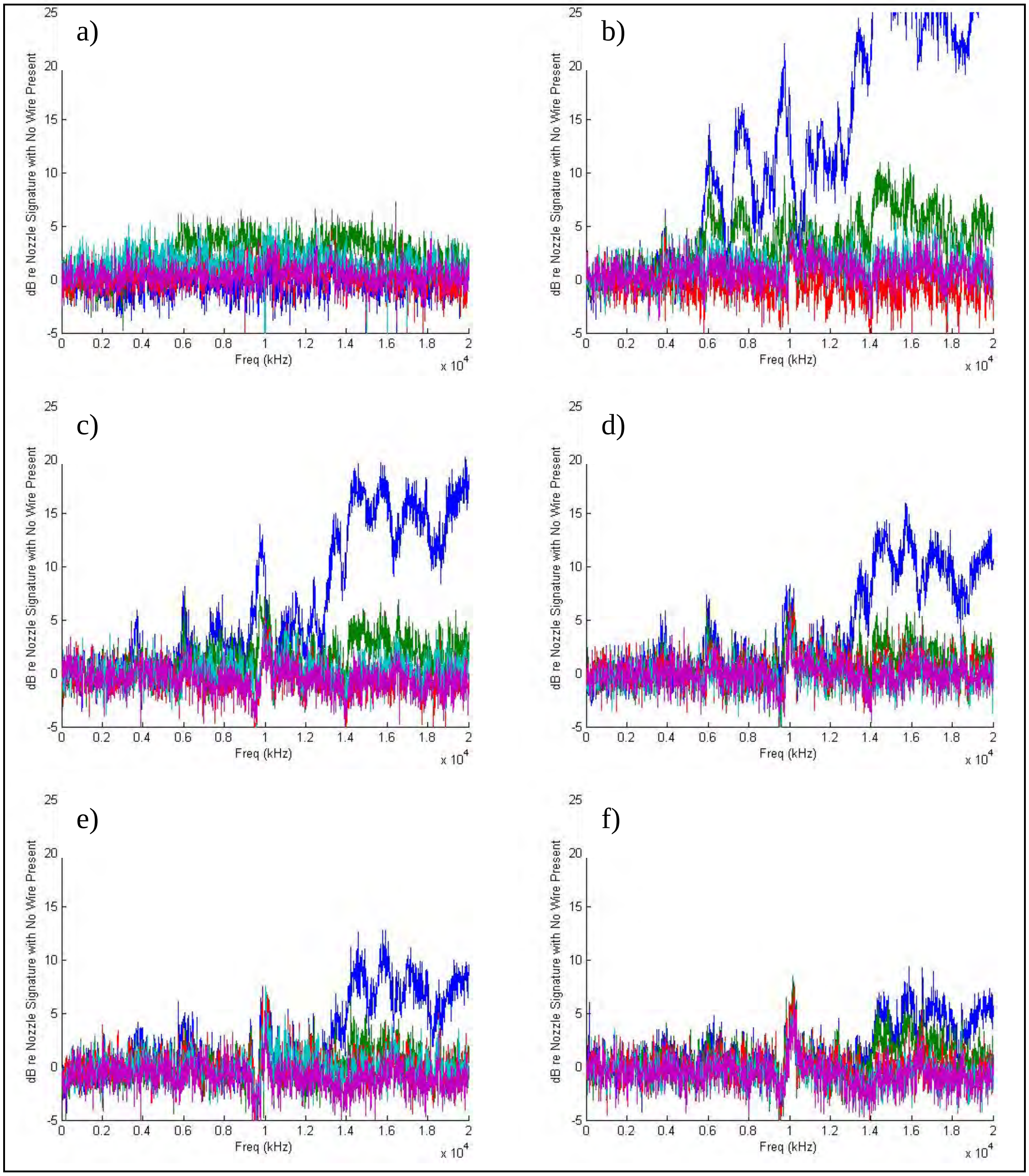

Figure A-2. 7-hole nozzle with round nylon fishing line, zero tension, microphone at 90° (a) 10 scfh, (b) 20 scfh, (c) 30 scfh, (d) 40 scfh, (e) 50 scfh, and (f) 60 scfh. Color representation as in figure 5.

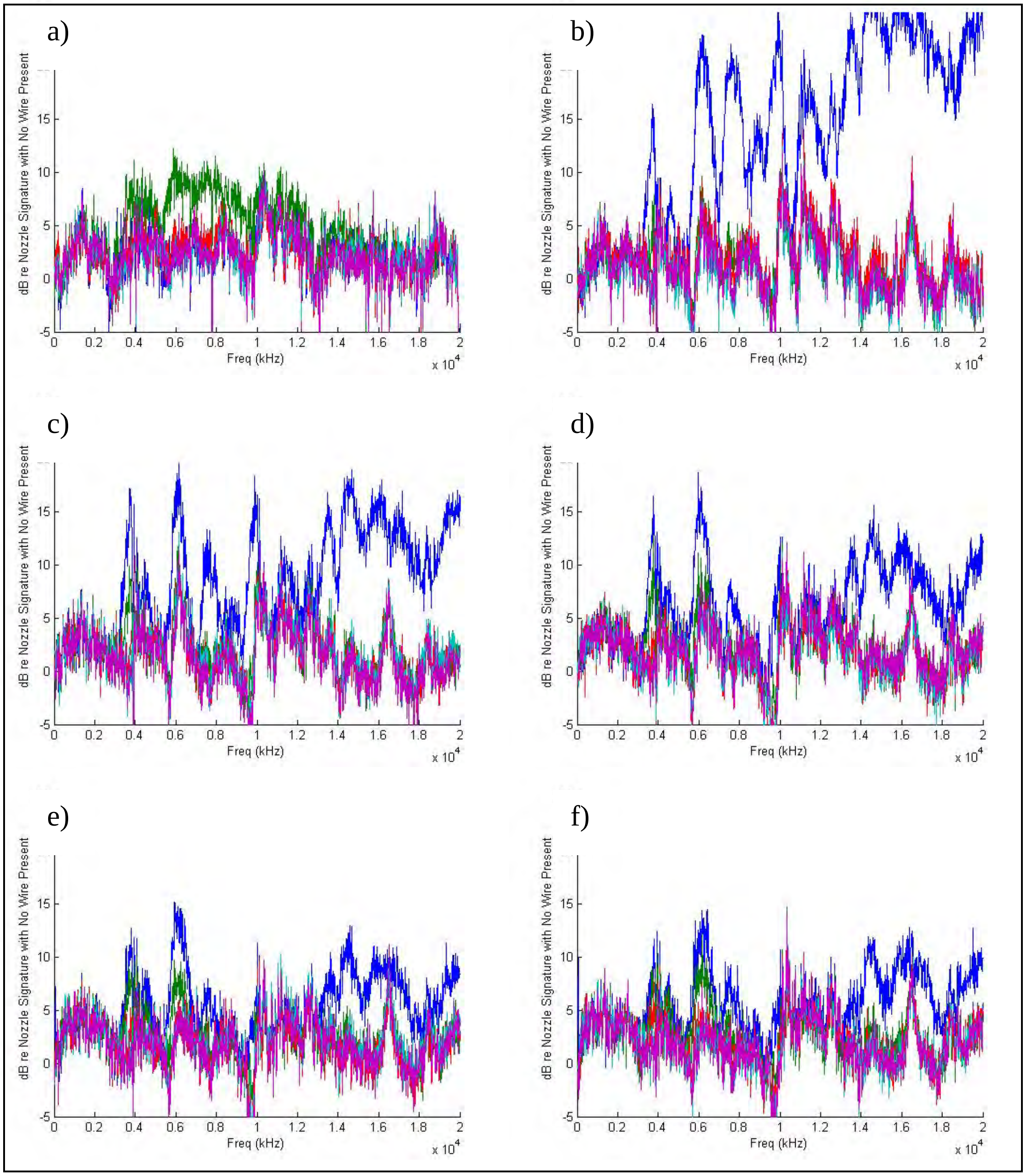

Figure A-3. 7-hole nozzle with non-insulated mild steel wire, zero tension, microphone at 90° (a) 10 scfh, (b) 20 scfh, (c) 30 scfh, (d) 40 scfh, (e) 50 scfh, and (f) 60 scfh. Color representation as in figure 5.

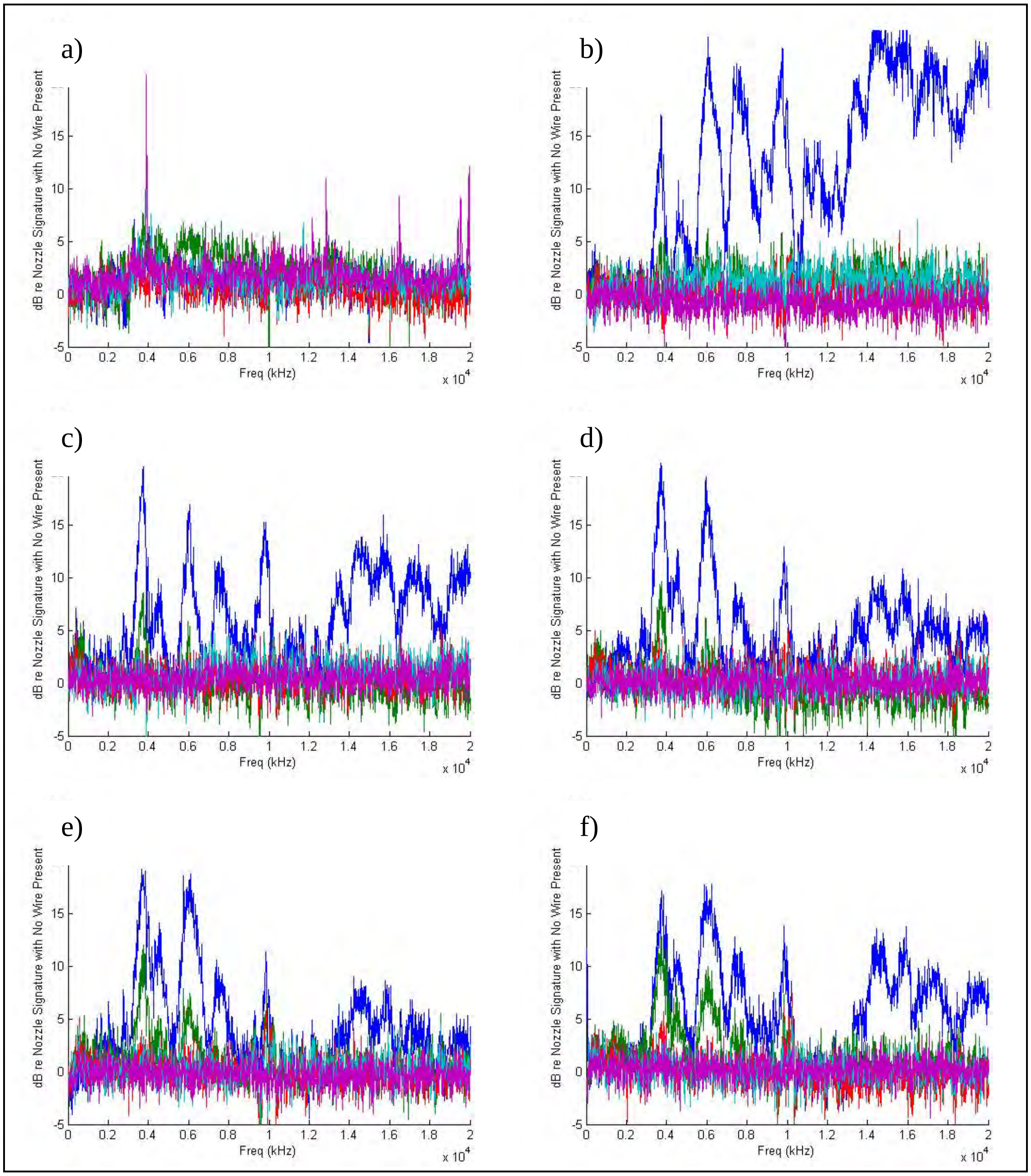

Figure A-4. 7-hole nozzle with white cotton string, zero tension, microphone at 90° (a) 10 scfh, (b) 20 scfh, (c) 30 scfh, (d) 40 scfh, (e) 50 scfh, and (f) 60 scfh. Color representation as in figure 5.

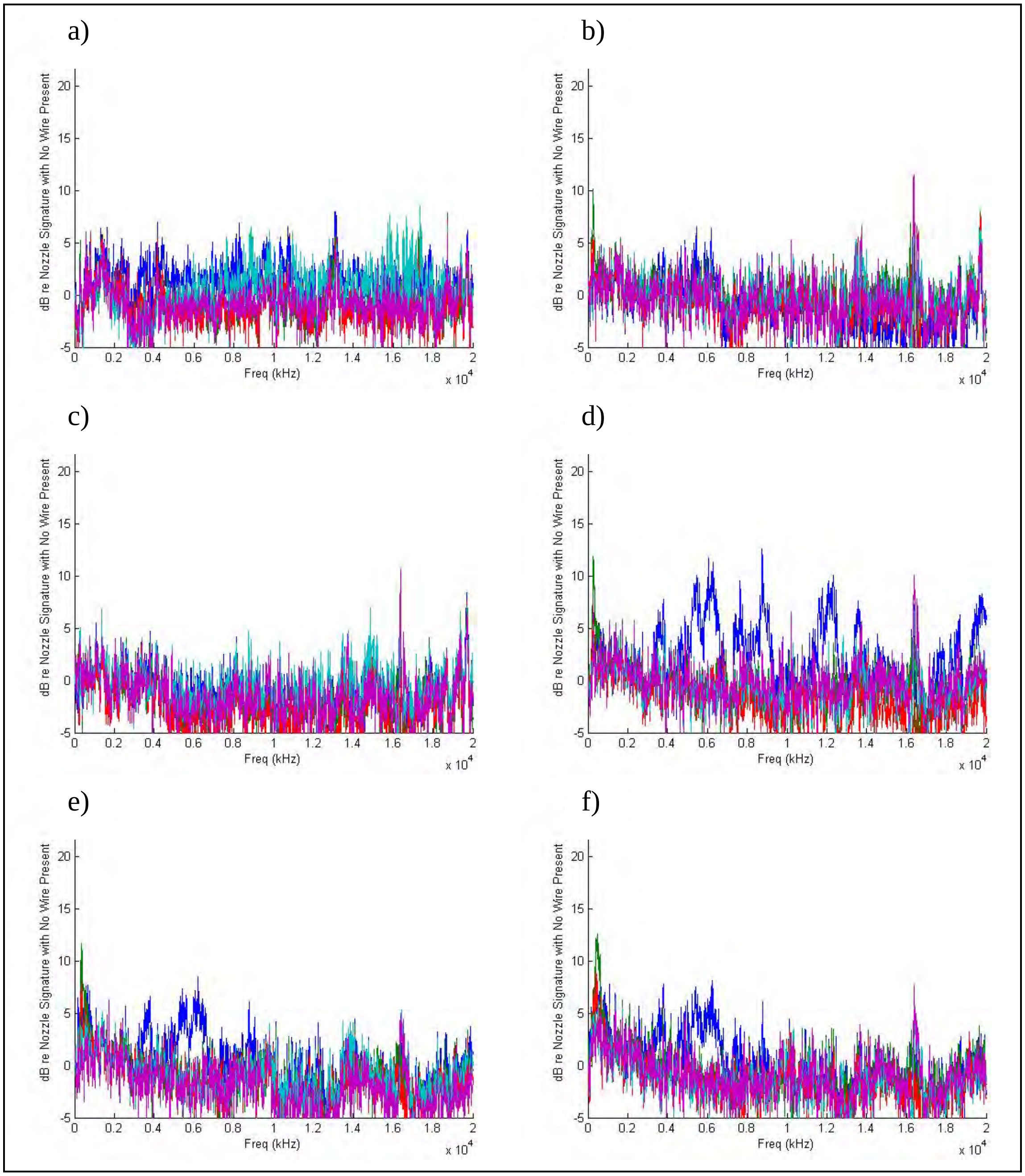

Figure A-5. 19-hole nozzle with 1 conductor speaker wire, zero tension, microphone at 90° (a) 10 scfh, (b) 20 scfh, (c) 30 scfh, (d) 40 scfh, (e) 50 scfh, and (f) 60 scfh. Color representation as in figure 5.

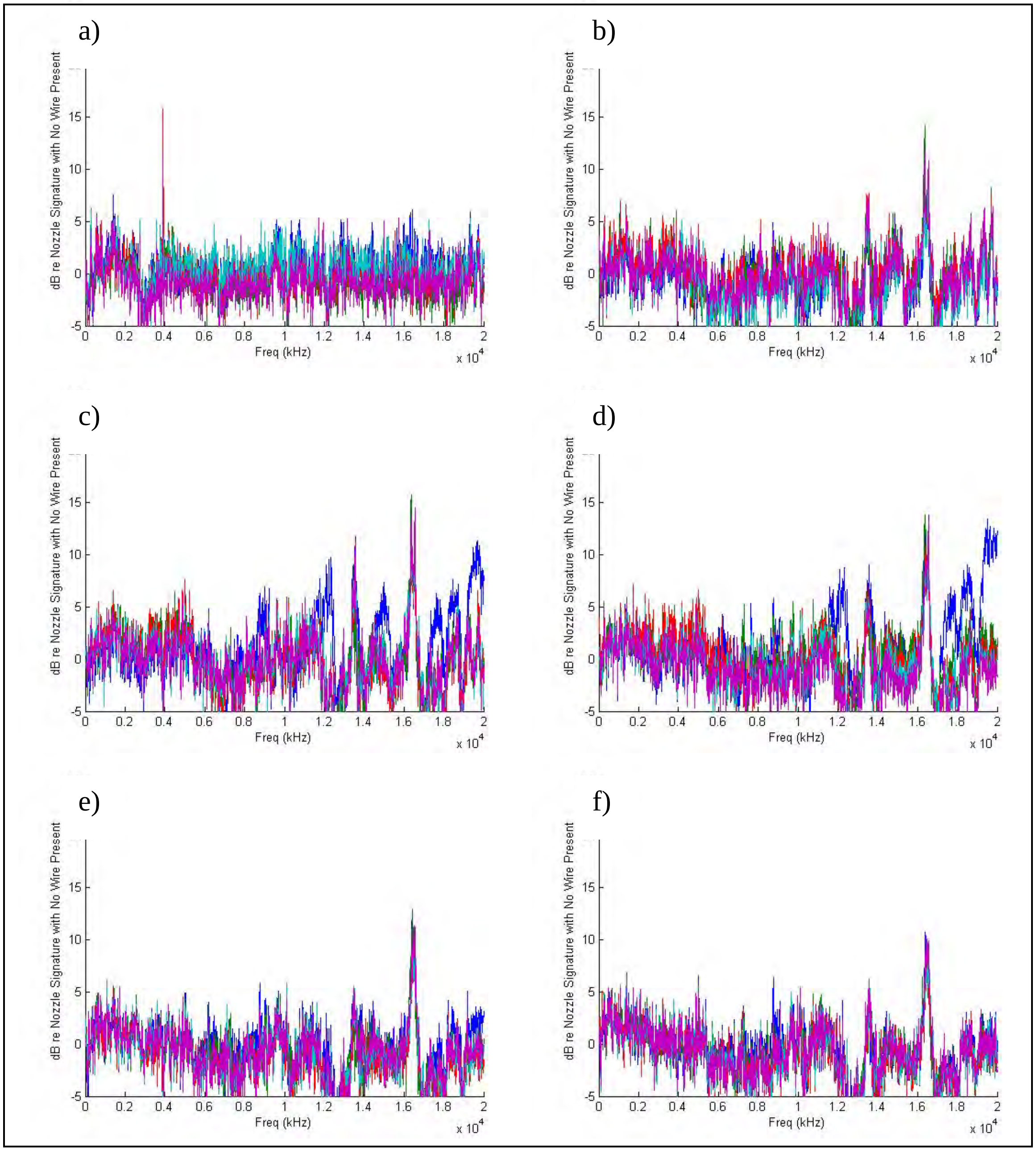

Figure A-6. 19-hole nozzle with round nylon fishing line, zero tension, microphone at 90° (a) 10 scfh, (b) 20 scfh, (c) 30 scfh, (d) 40 scfh, (e) 50 scfh, and (f) 60 scfh. Color representation as in figure 5.

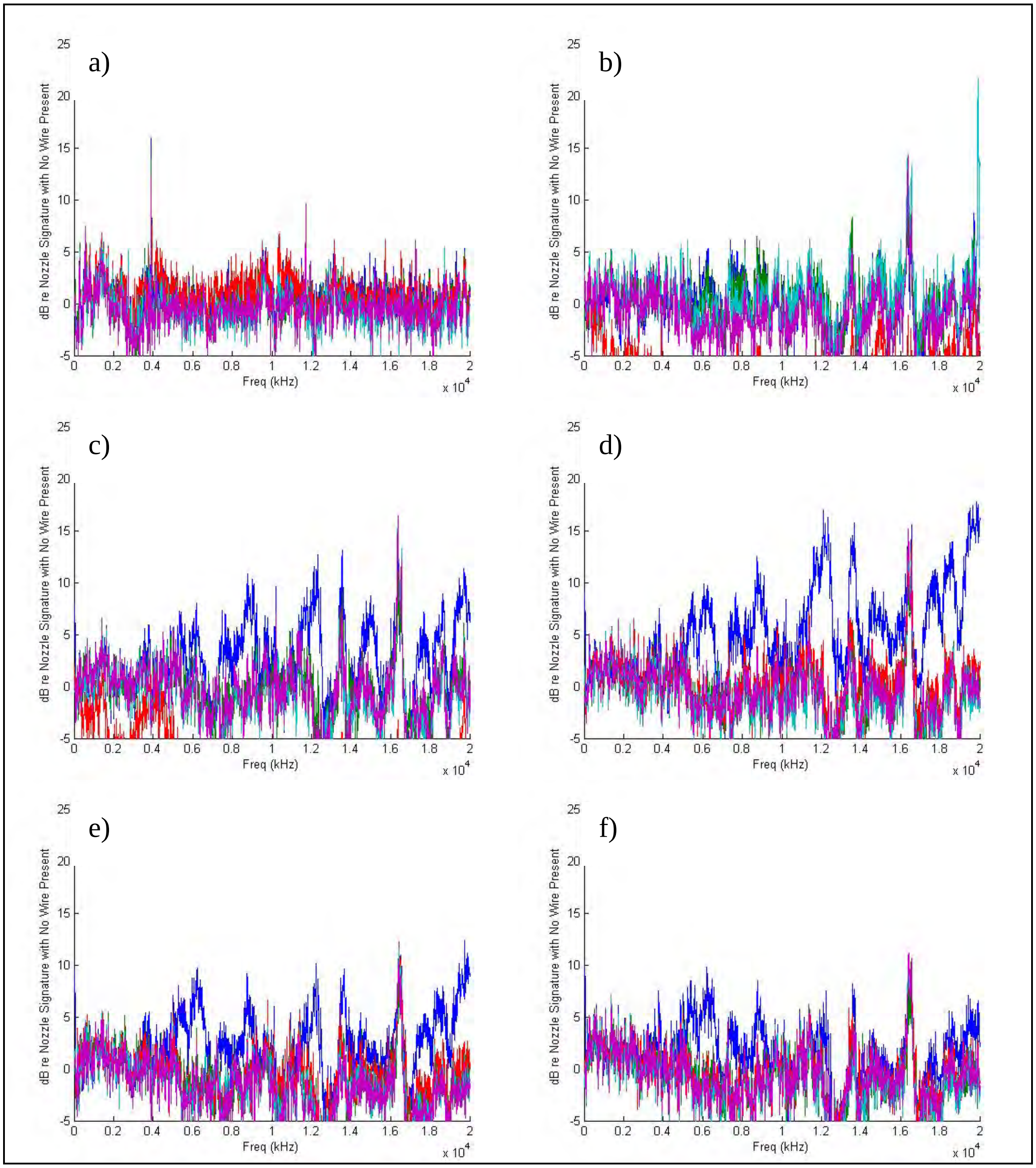

Figure A-7. 19-hole nozzle with non-insulated mild steel wire, zero tension, microphone at 90° (a) 10 scfh, (b) 20 scfh, (c) 30 scfh, (d) 40 scfh, (e) 50 scfh, and (f) 60 scfh. Color representation as in figure 5.

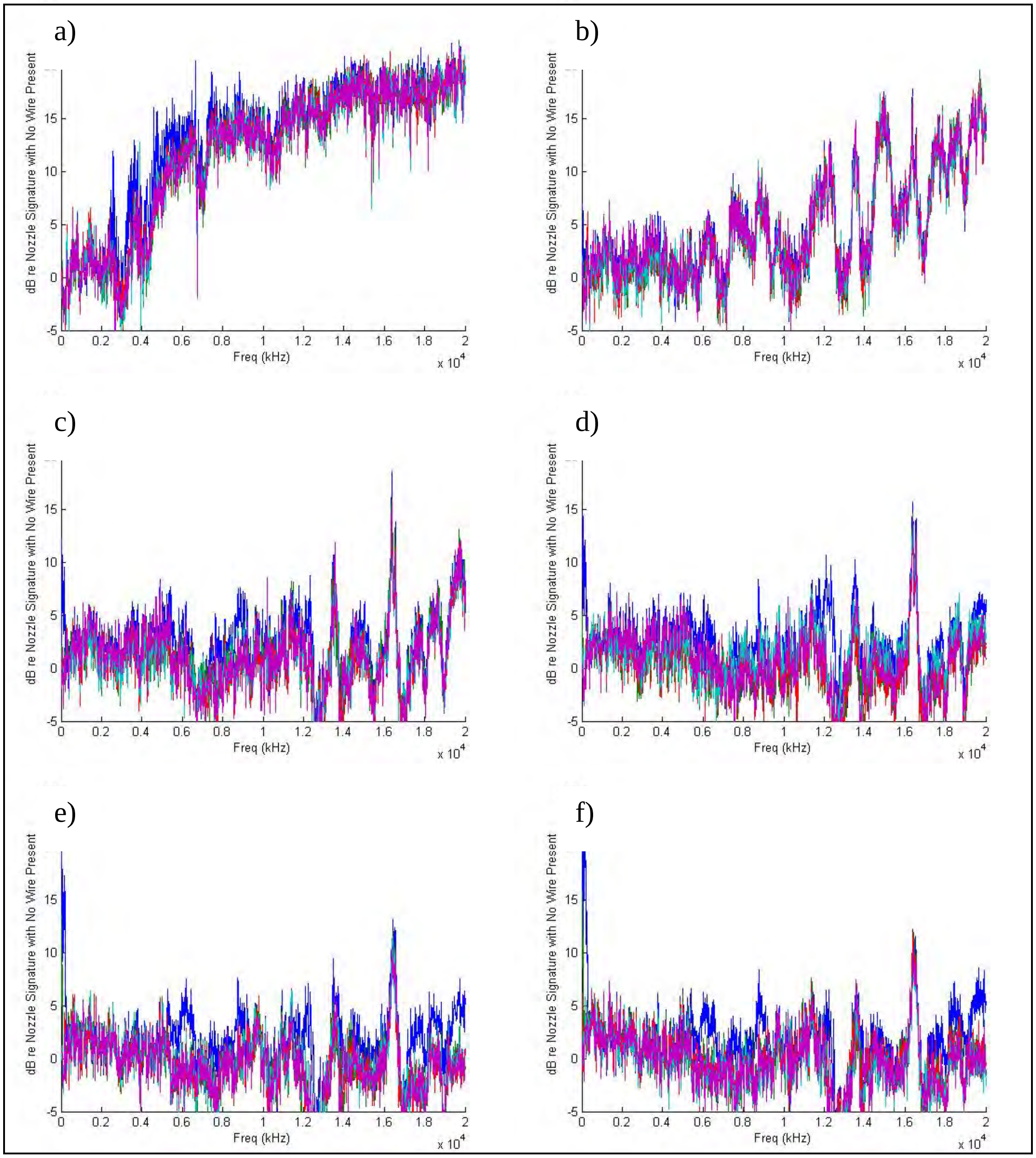

Figure A-8. 19-hole nozzle with white cotton string, zero tension, microphone at 90° (a) 10 scfh, (b) 20 scfh, (c) 30 scfh, (d) 40 scfh, (e) 50 scfh, and (f) 60 scfh. Color representation as in figure 5.

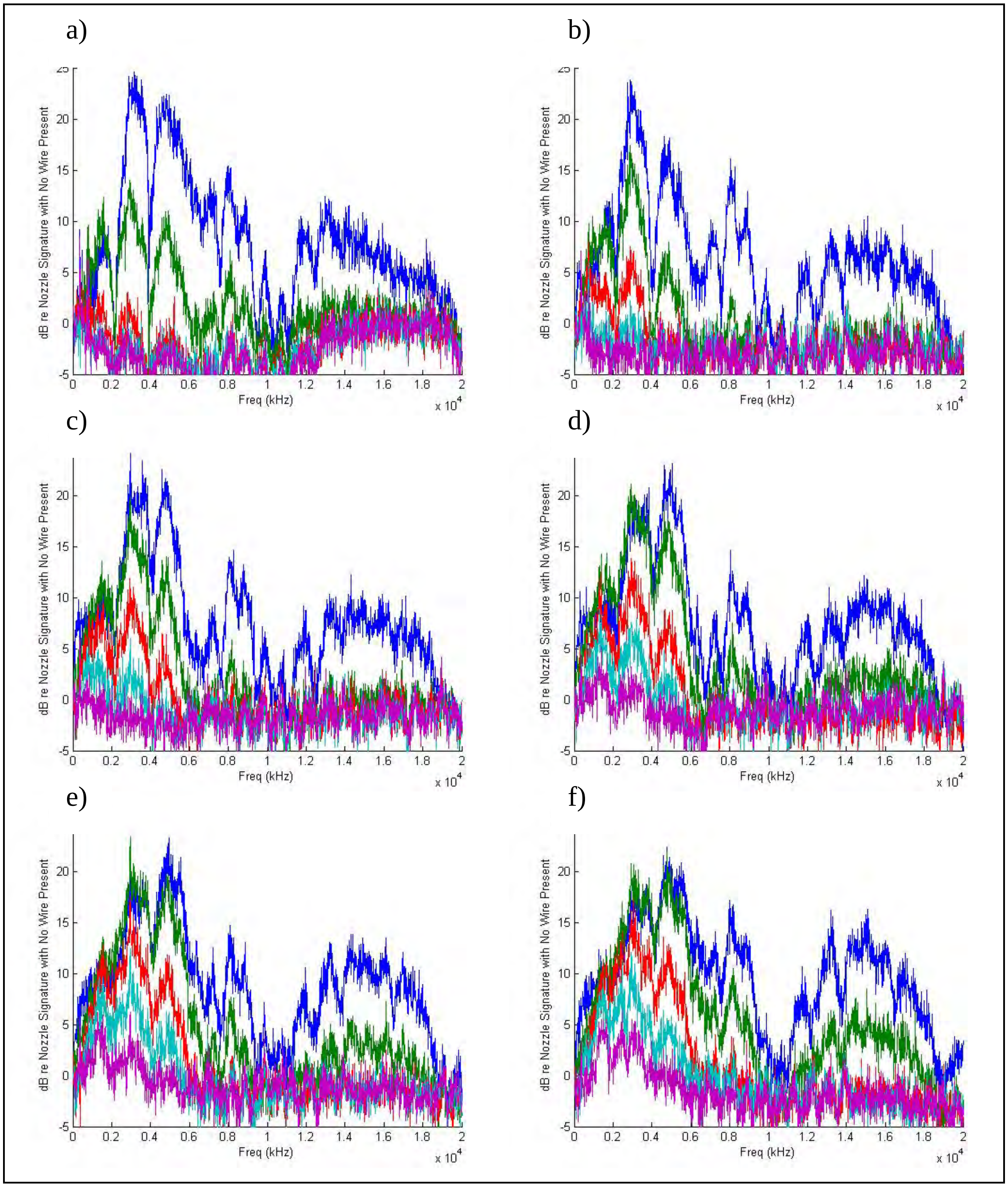

Figure A-9. Single-hole nozzle 1 conductor speaker wire, zero tension, microphone at 90° (a) 10 scfh, (b) 20 scfh, (c) 30 scfh, (d) 40 scfh, (e) 50 scfh, and (f) 60 scfh. Color representation as in figure 5.

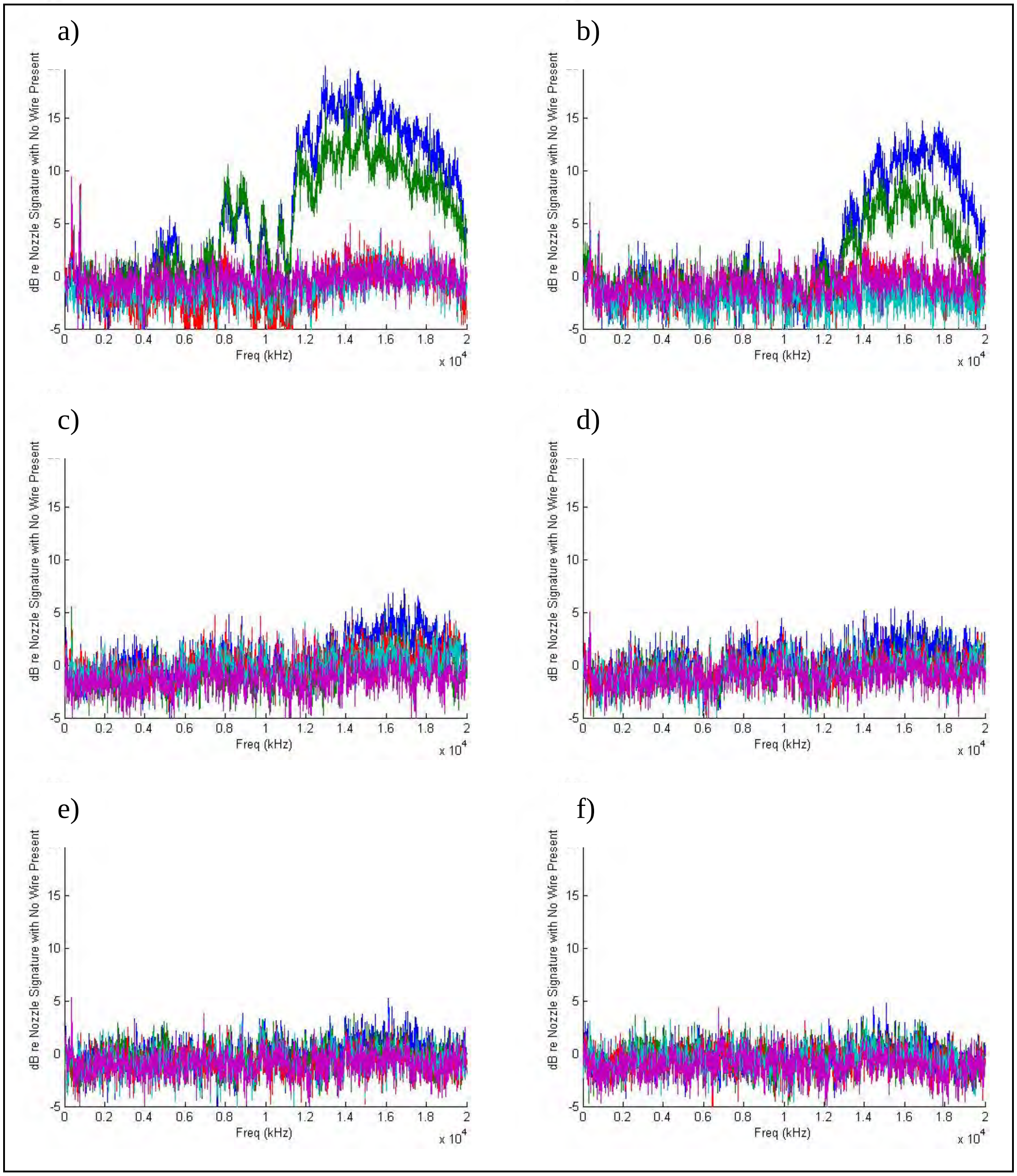

Figure A-10. Single-hole nozzle round nylon fishing line, zero tension, microphone at 90° (a) 10 scfh, (b) 20 scfh, (c) 30 scfh, (d) 40 scfh, (e) 50 scfh, and (f) 60 scfh. Color representation as in figure 5.

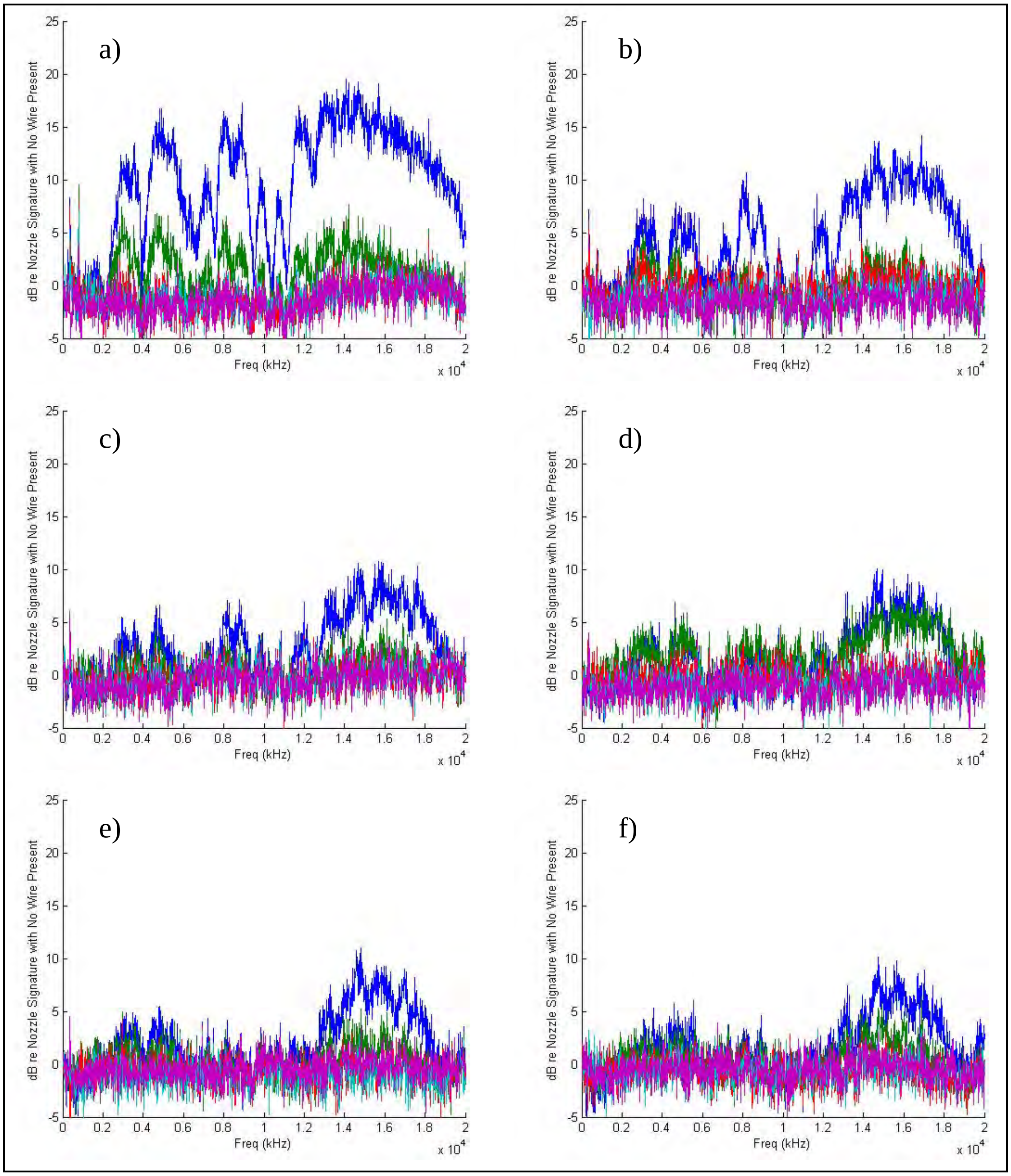

Figure A-11. Single-hole nozzle non-insulated mild steel wire, zero tension, microphone at 90^{o} (a) 10 scfh, (b) 20 scfh, (c) 30 scfh, (d) 40 scfh, (e) 50 scfh, and (f) 60 scfh. Color representation as in figure 5.

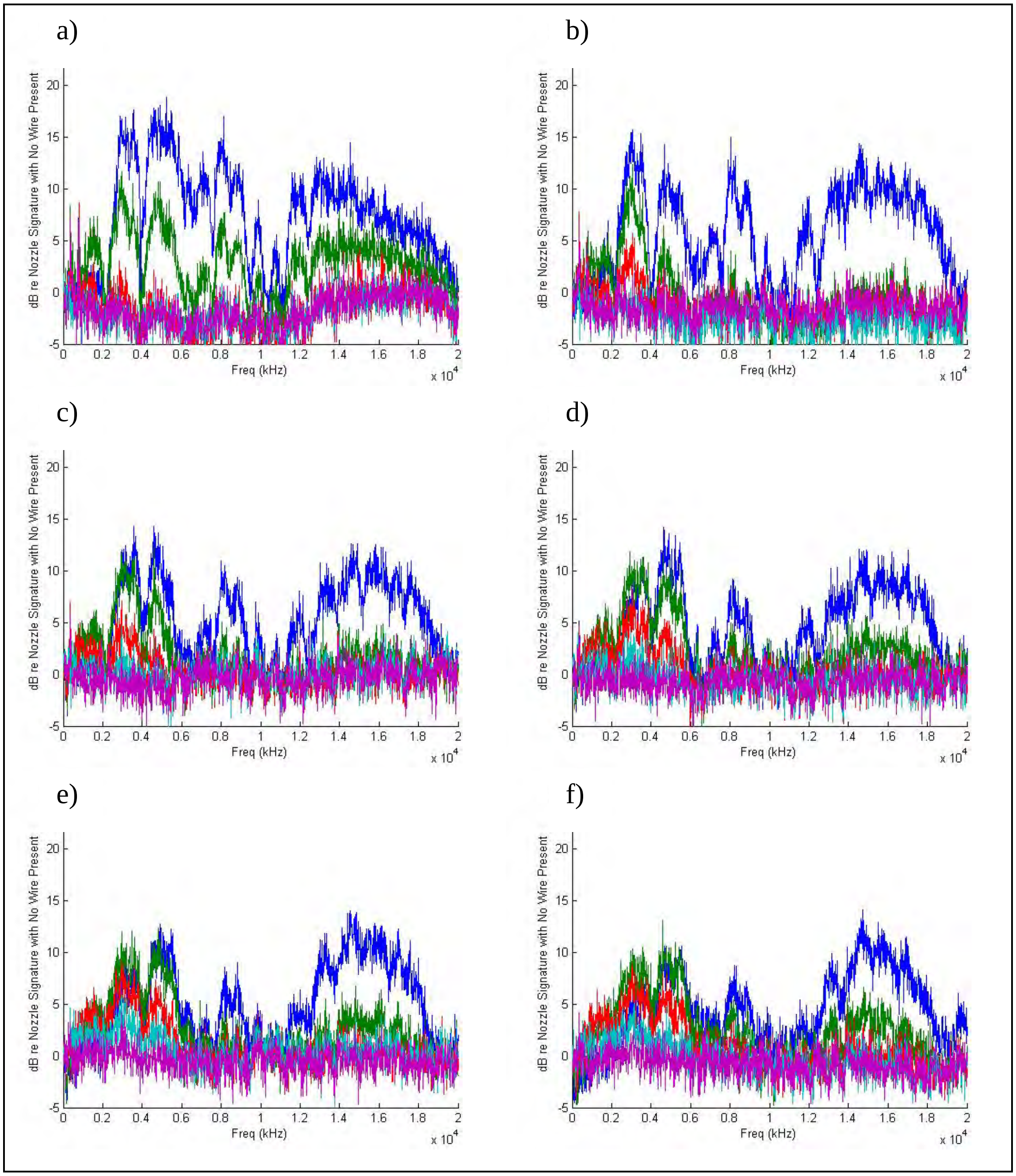

Figure A-12. Single-hole nozzle with white cotton string, zero tension, microphone at 90° (a) 10 scfh, (b) 20 scfh, (c) 30 scfh, (d) 40 scfh, (e) 50 scfh, and (f) 60 scfh. Color representation as in figure 5.

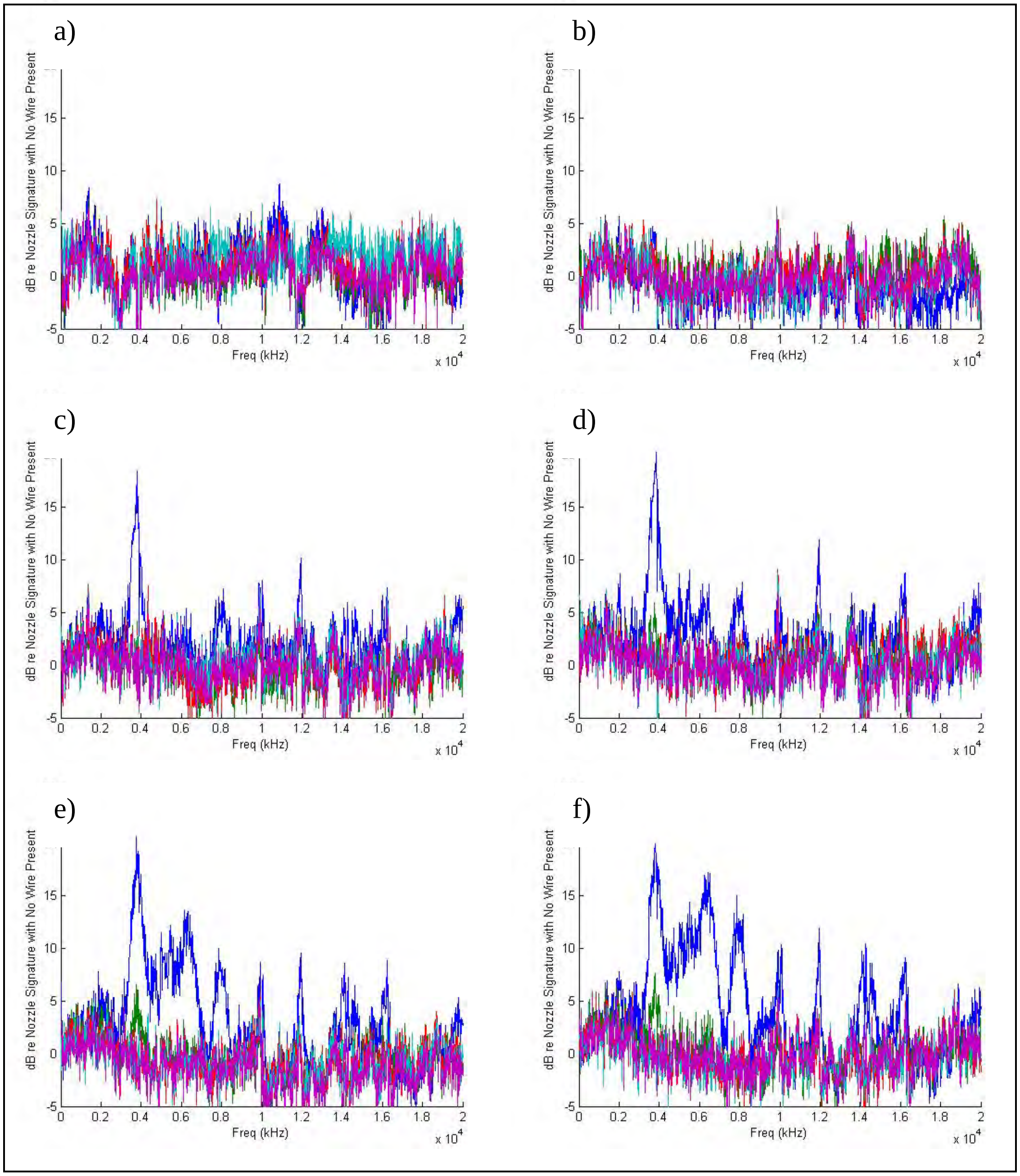

Figure A-13. Slit nozzle with 1 conductor speaker wire, zero tension, microphone at 90° (a) 10 scfh, (b) 20 scfh, (c) 30 scfh, (d) 40 scfh, (e) 50 scfh, and (f) 60 scfh. Color representation as in figure 5.

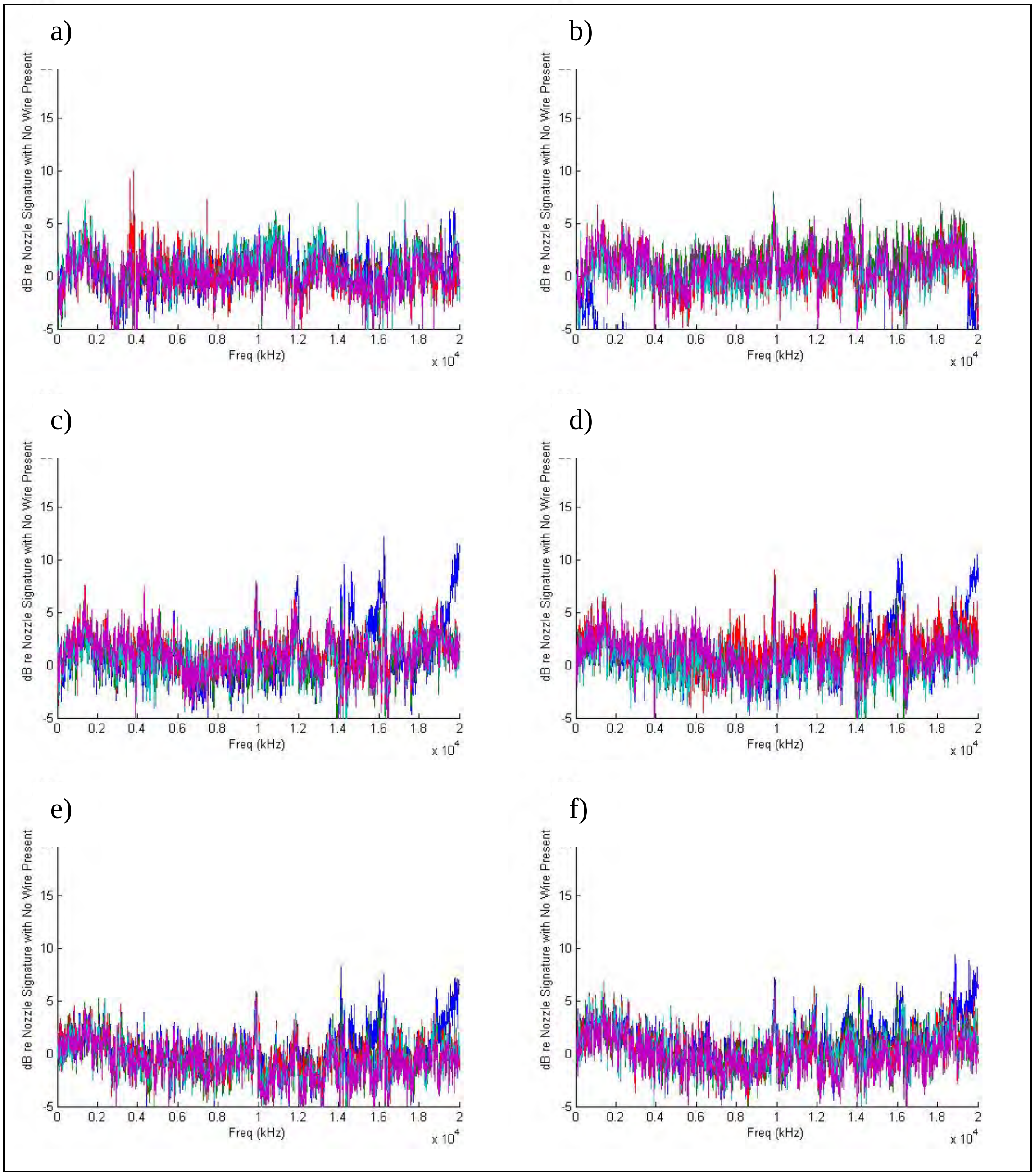

Figure A-14. Slit nozzle with round nylon fishing line, zero tension, microphone at 90° (a) 10 scfh, (b) 20 scfh, (c) 30 scfh, (d) 40 scfh, (e) 50 scfh, and (f) 60 scfh. Color representation as in figure 5.

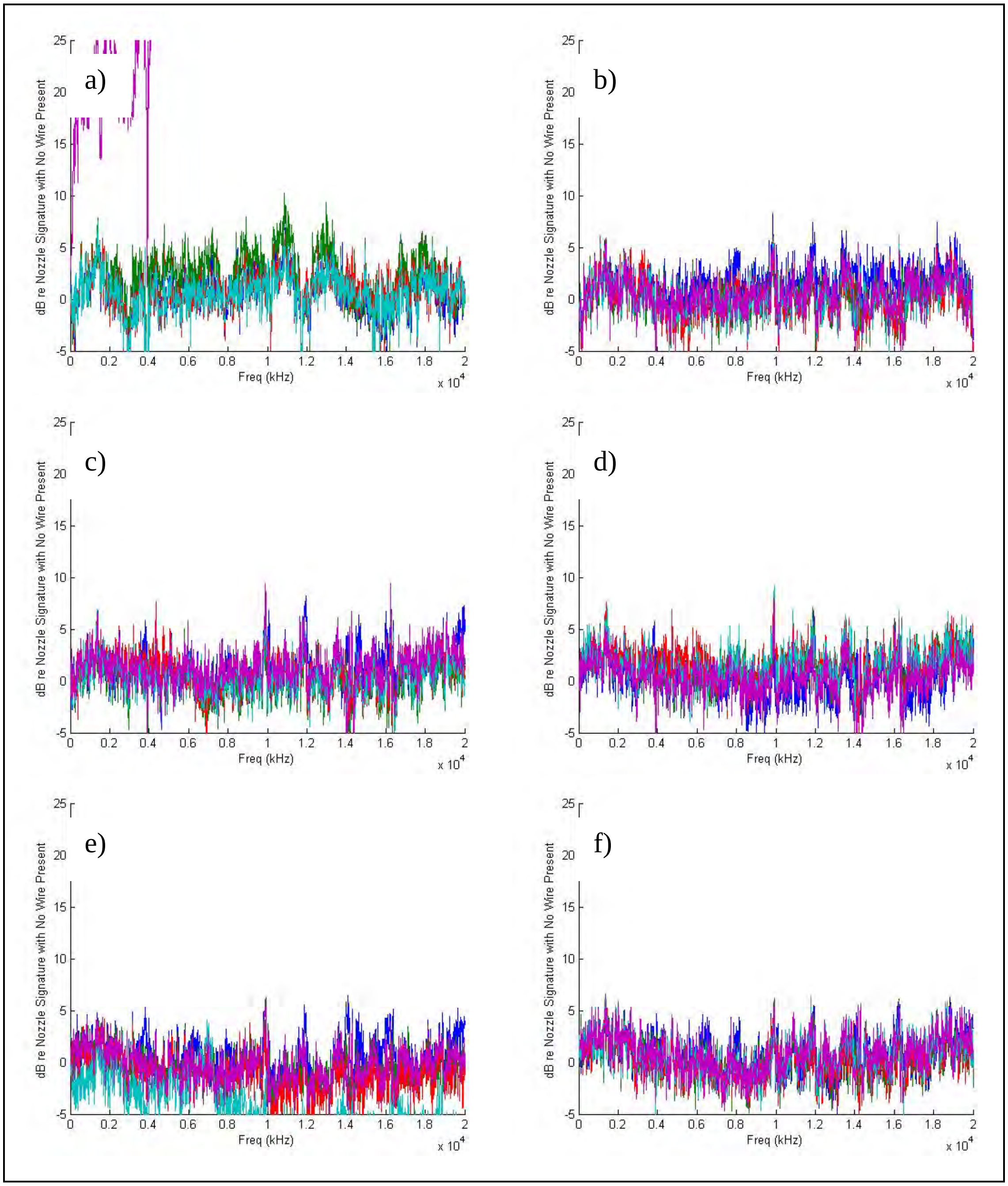

Figure A-15. Slit nozzle with non-insulated mild steel wire, zero tension, microphone at 90° (a) 10 scfh, (b) 20 scfh, (c) 30 scfh, (d) 40 scfh, (e) 50 scfh, and (f) 60 scfh. Color representation as in figure 5.

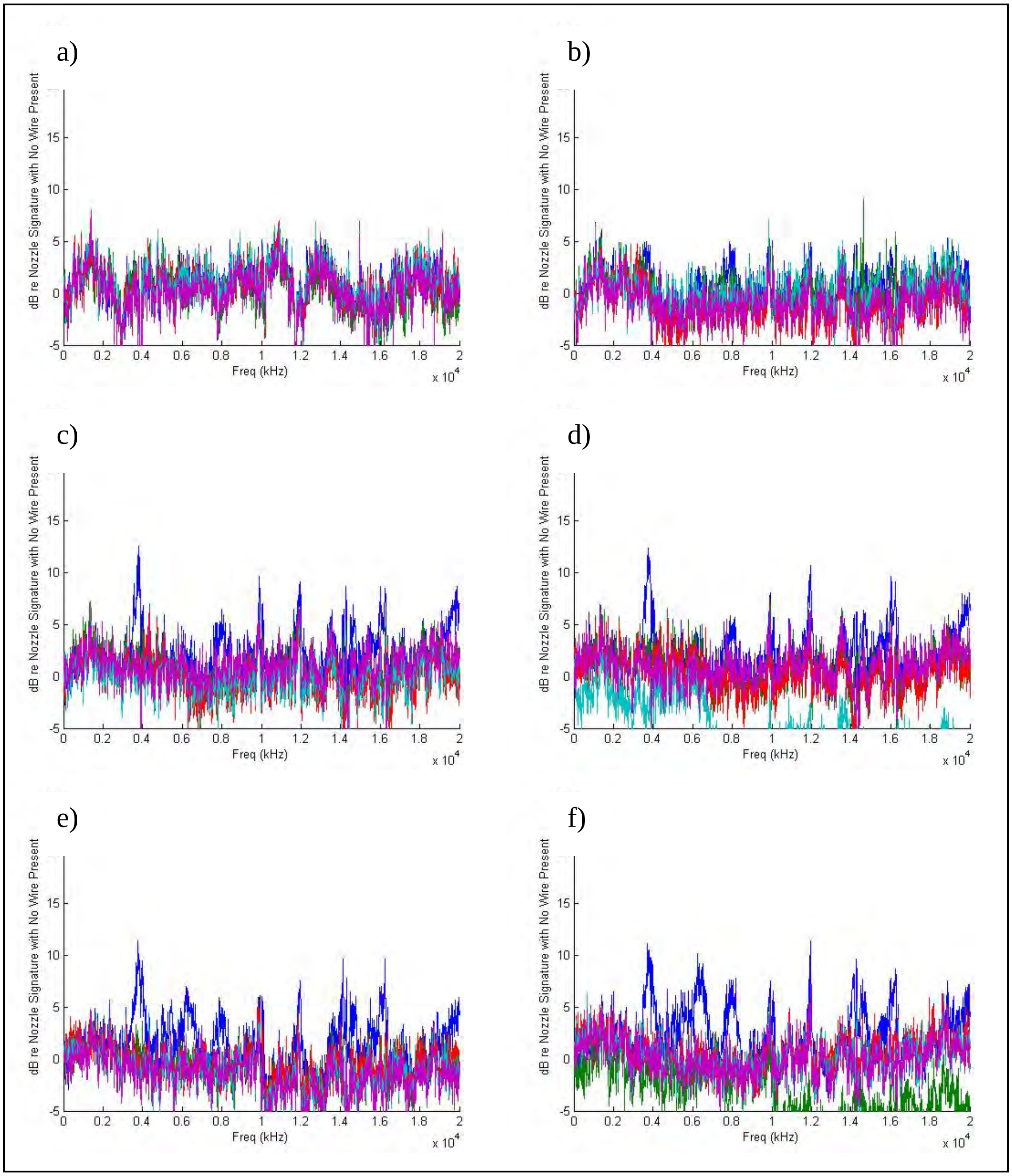

Figure A-16. Slit nozzle with white cotton string, zero tension, microphone at 90° (a) 10 scfh, (b) 20 scfh, (c) 30 scfh, (d) 40 scfh, (e) 50 scfh, and (f) 60 scfh. Color representation as in figure 5.

Appendix B. Single-hole Nozzle with Wires at Different Tensions

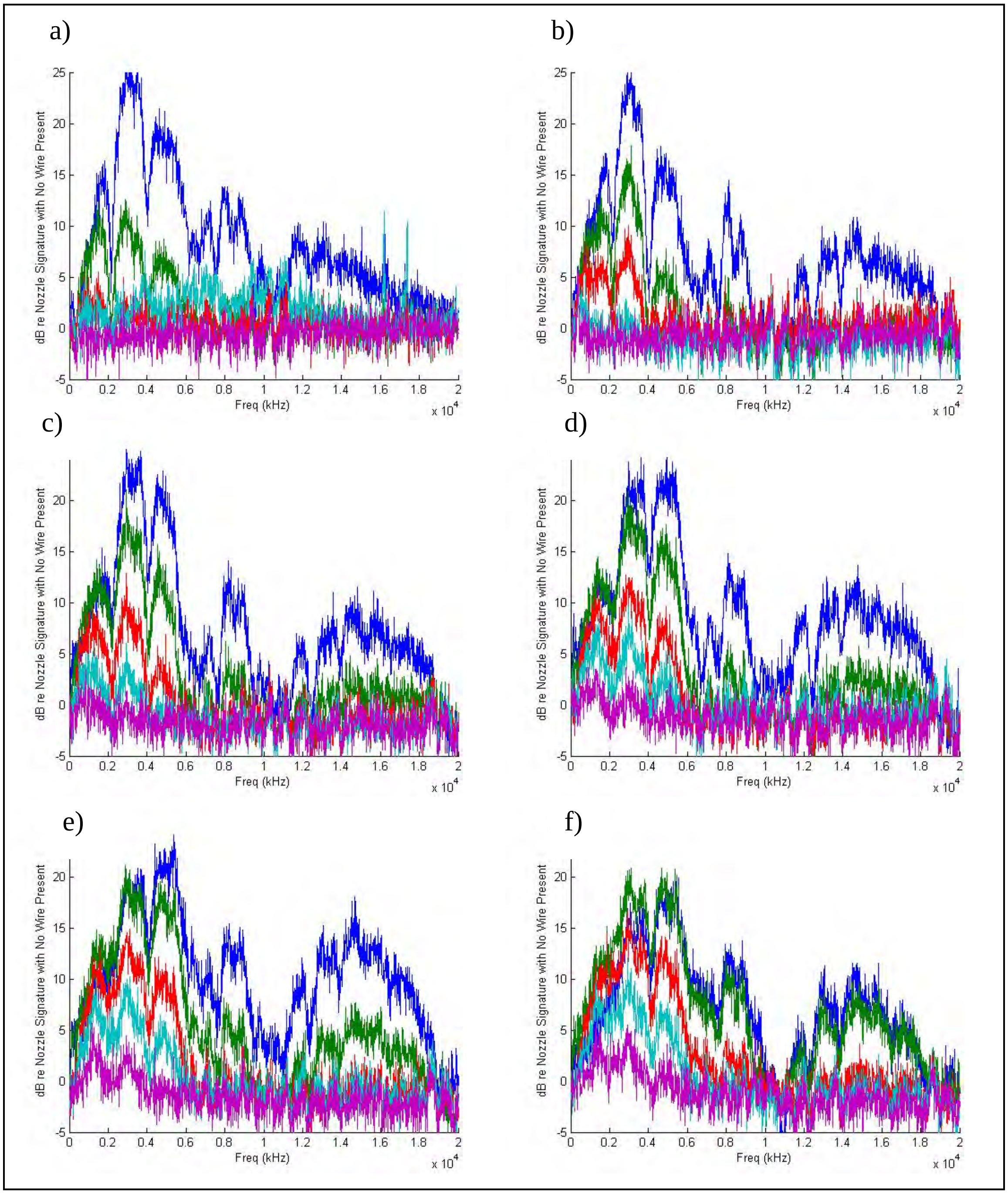

Figure B-1. 1 conductor speaker wire .5 kg tension; single-hole nozzle; microphone at 0° (a) 10 scfh, (b) 20 scfh, (c) 30 scfh, (d) 40 scfh, (e) 50 scfh, and (f) 60 scfh. Color representation as in figure 5.

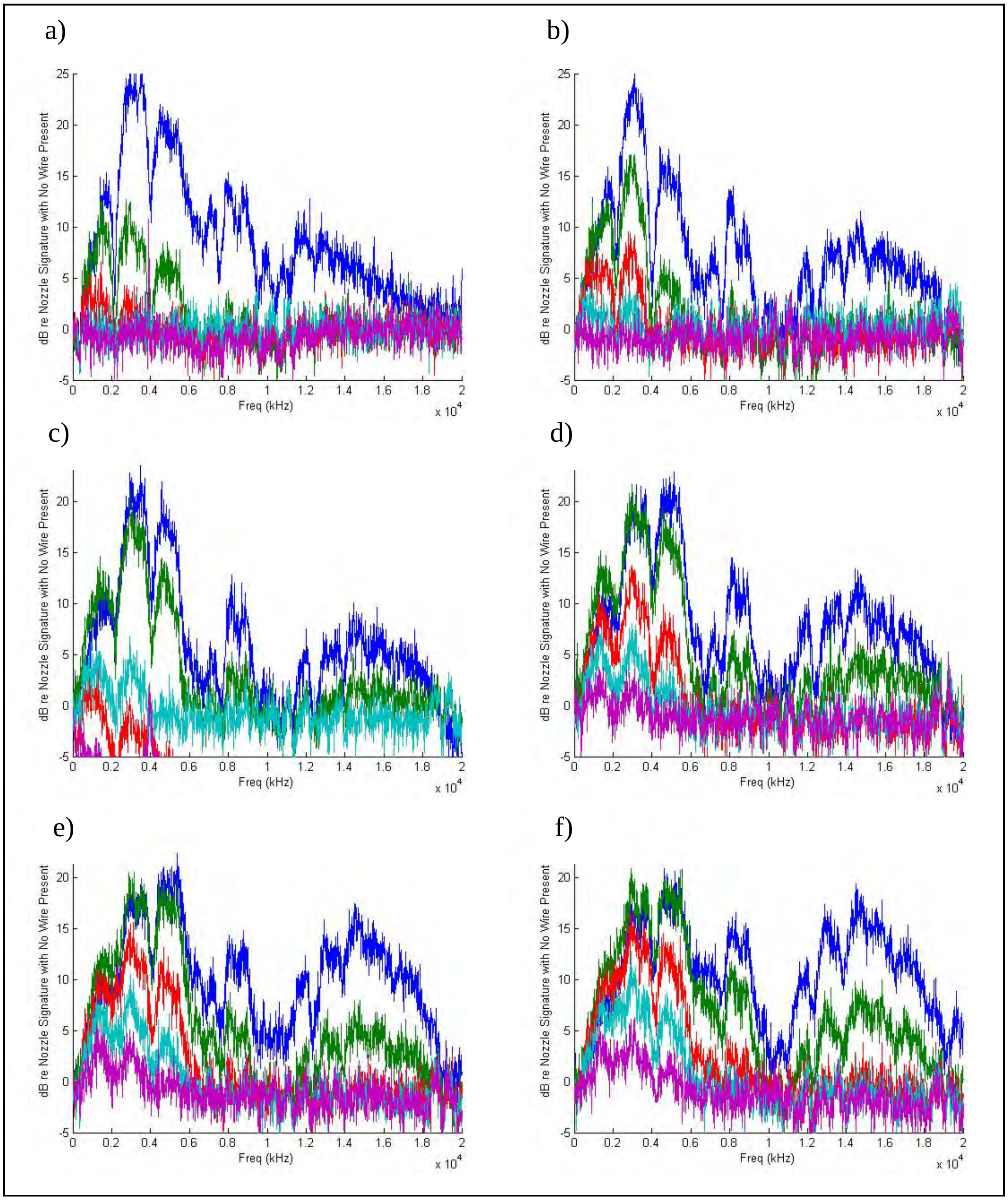

Figure B-2. 1 conductor speaker wire 1.0 kg tension; single-hole nozzle; microphone at 0° (a) 10 scfh, (b) 20 scfh, (c) 30 scfh, (d) 40 scfh, (e) 50 scfh, and (f) 60 scfh. Color representation as in figure 5.

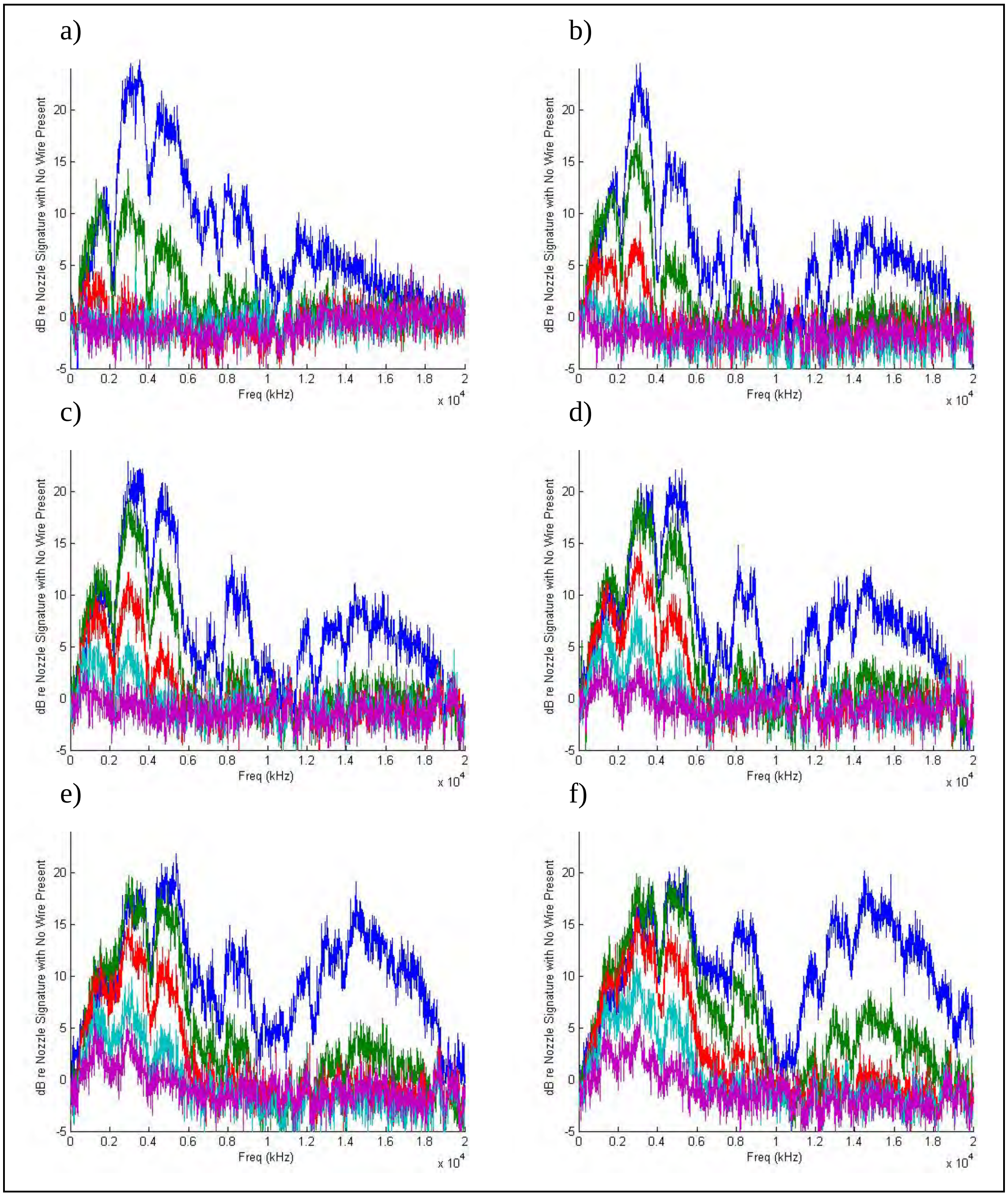

Figure B-3. 1 conductor speaker wire 1.5 kg tension; single-hole nozzle; microphone at 0° (a) 10 scfh, (b) 20 scfh, (c) 30 scfh, (d) 40 scfh, (e) 50 scfh, and (f) 60 scfh. Color representation as in figure 5.

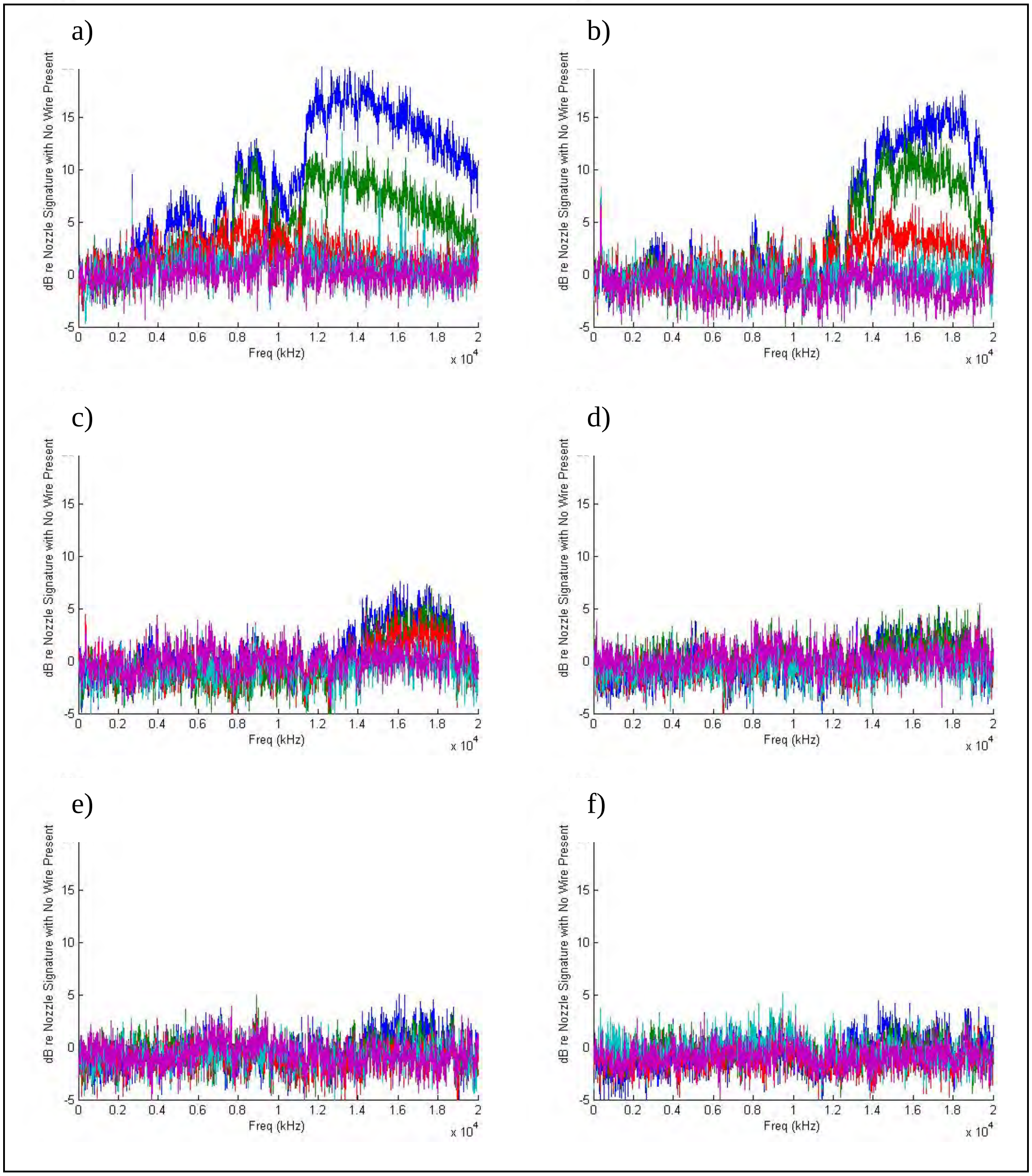

Figure B-4. Round nylon fishing line .5 kg tension; single-hole nozzle; microphone at 0° (a) 10 scfh, (b) 20 scfh, (c) 30 scfh, (d) 40 scfh, (e) 50 scfh, and (f) 60 scfh. Color representation as in figure 5.

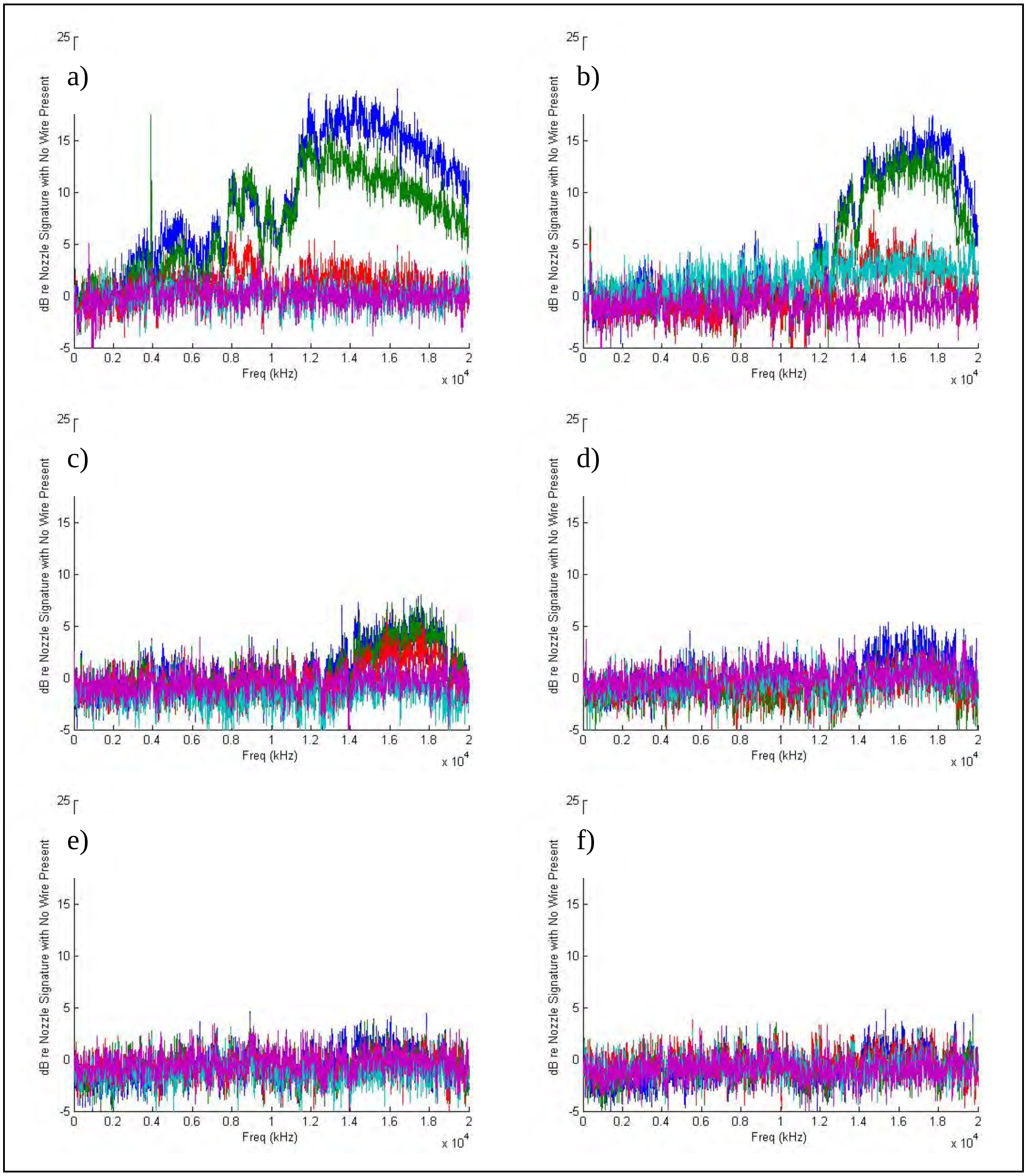

Figure B-5. Round nylon fishing line 1.0 kg tension; single-hole nozzle; microphone at 0° (a) 10 scfh, (b) 20 scfh, (c) 30 scfh, (d) 40 scfh, (e) 50 scfh, and (f) 60 scfh. Color representation as in figure 5.

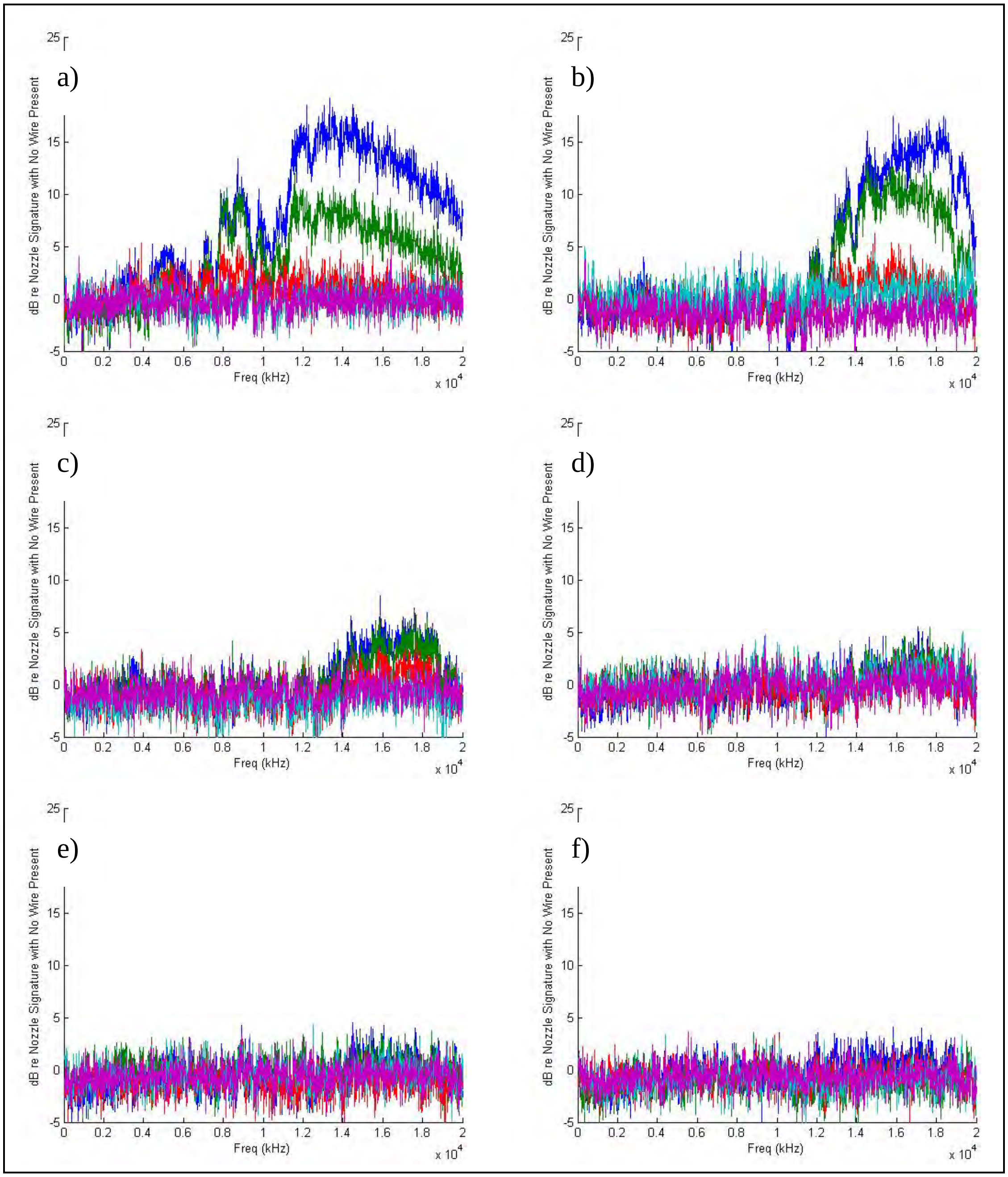

Figure B-6. Round nylon fishing line 1.5 kg tension; single-hole nozzle; microphone at 0° (a) 10 scfh, (b) 20 scfh, (c) 30 scfh, (d) 40 scfh, (e) 50 scfh, and (f) 60 scfh. Color representation as in figure 5.

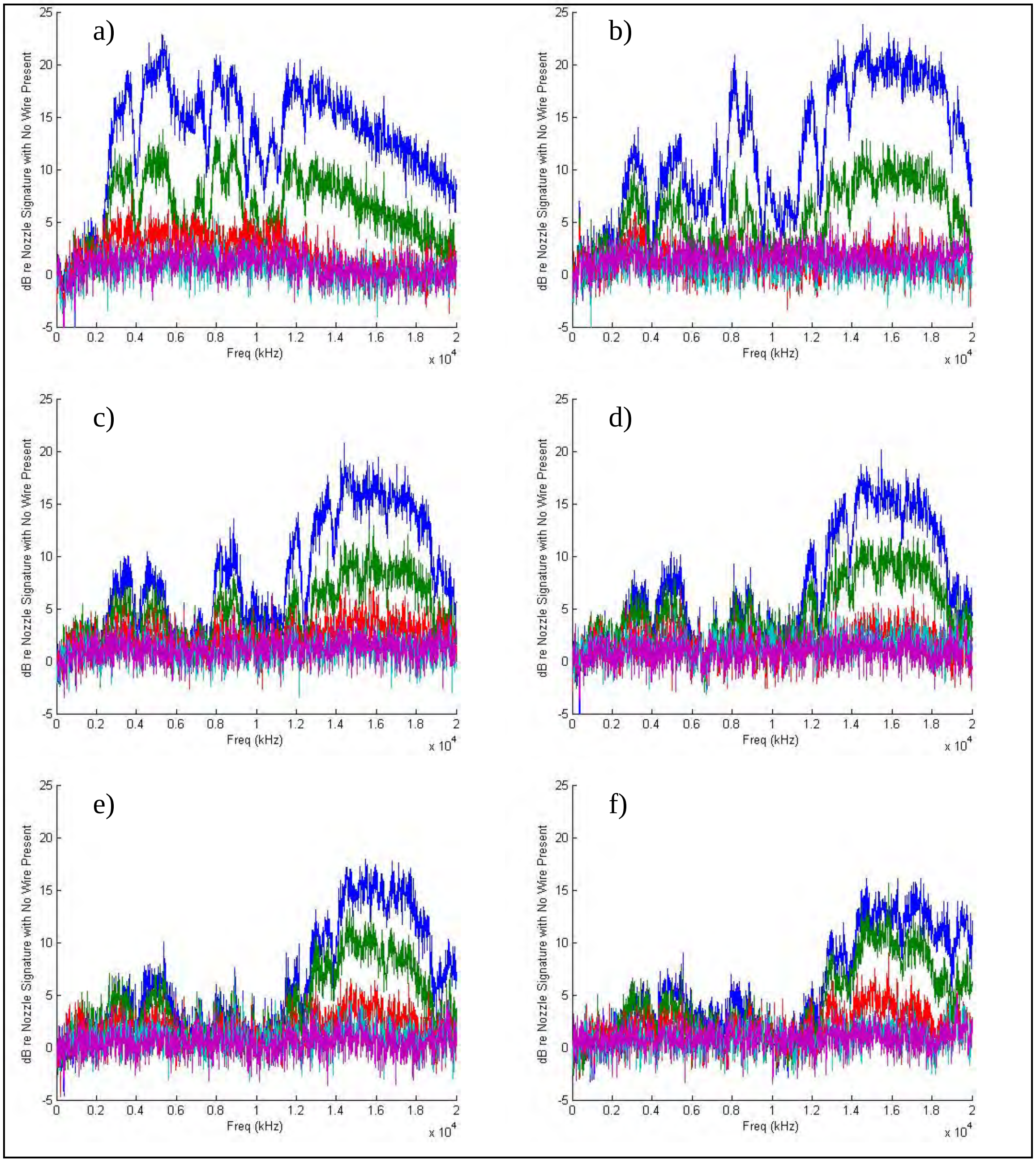

Figure B-7. Non-insulated mild steel wire .5 kg tension; single-hole nozzle; microphone at 0° (a) 10 scfh, (b) 20 scfh, (c) 30 scfh, (d) 40 scfh, (e) 50 scfh, and (f) 60 scfh. Color representation as in figure 5.

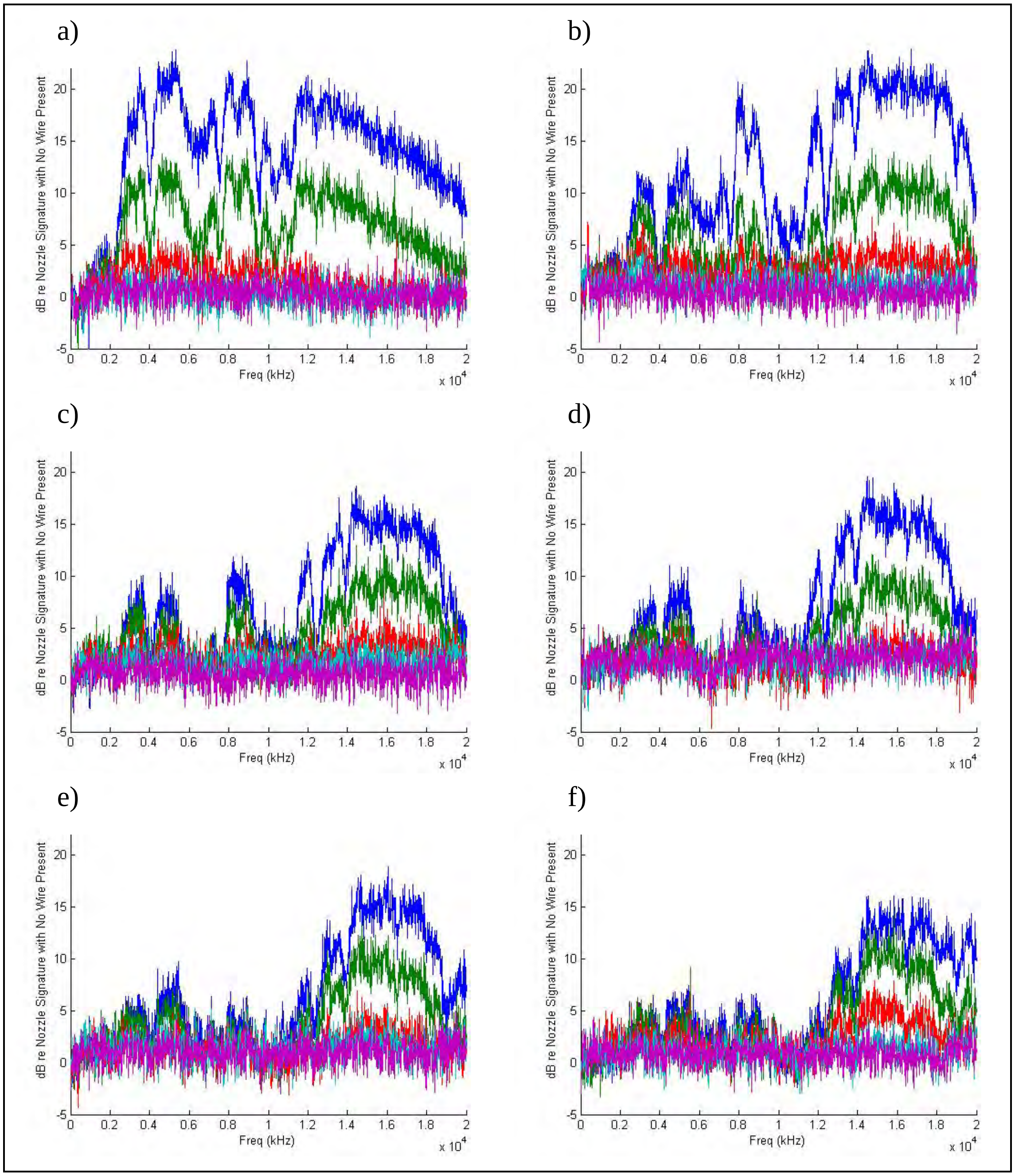

Figure B-8. Non-insulated mild steel wire 1.0 kg tension; single-hole nozzle; microphone at 0° (a) 10 scfh, (b) 20 scfh, (c) 30 scfh, (d) 40 scfh, (e) 50 scfh, and (f) 60 scfh. Color representation as in figure 5.

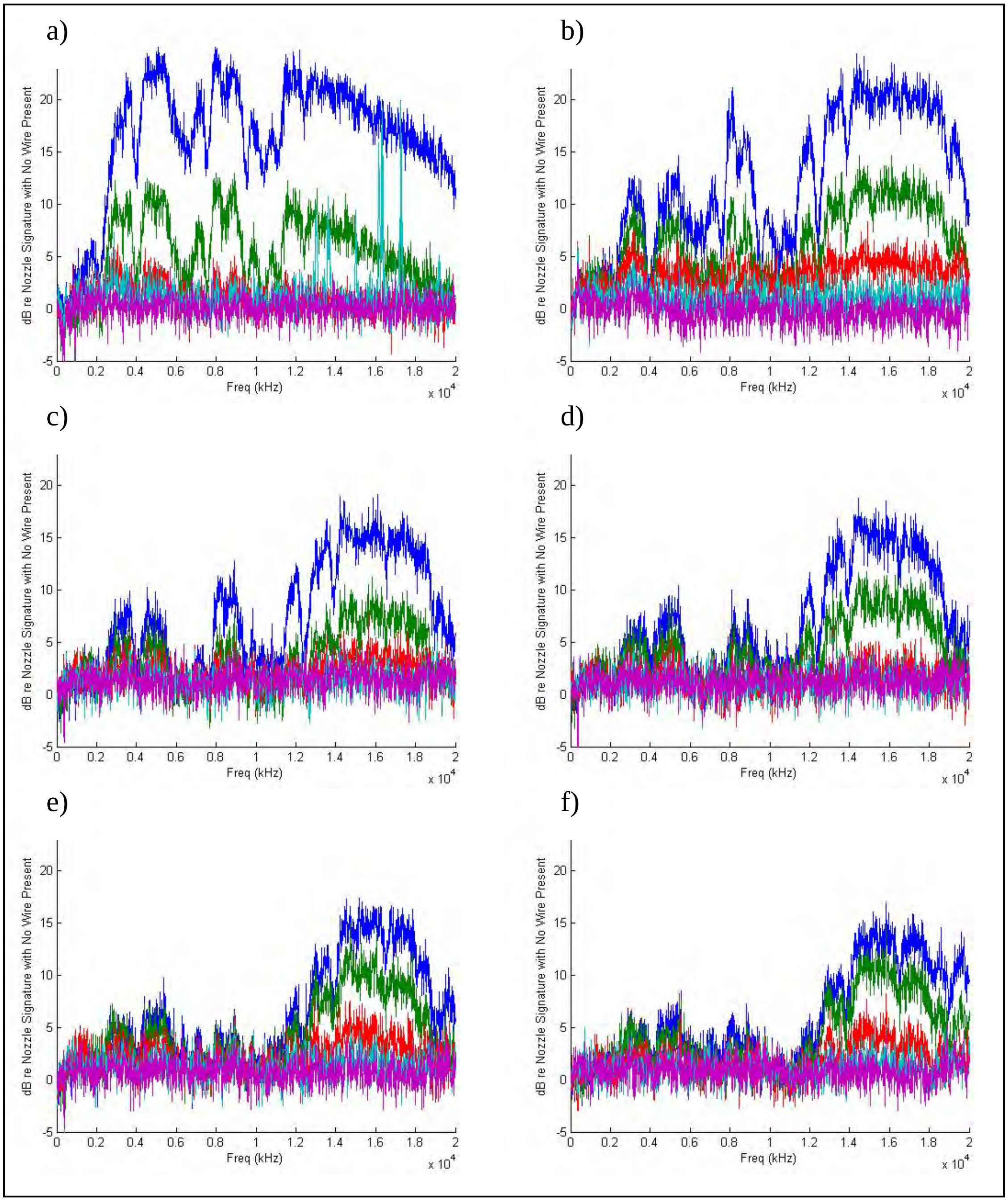

Figure B-9. Non-insulated mild steel wire 1.5 kg tension; single-hole nozzle; microphone at 0° (a) 10 scfh, (b) 20 scfh, (c) 30 scfh, (d) 40 scfh, (e) 50 scfh, and (f) 60 scfh. Color representation as in figure 5.

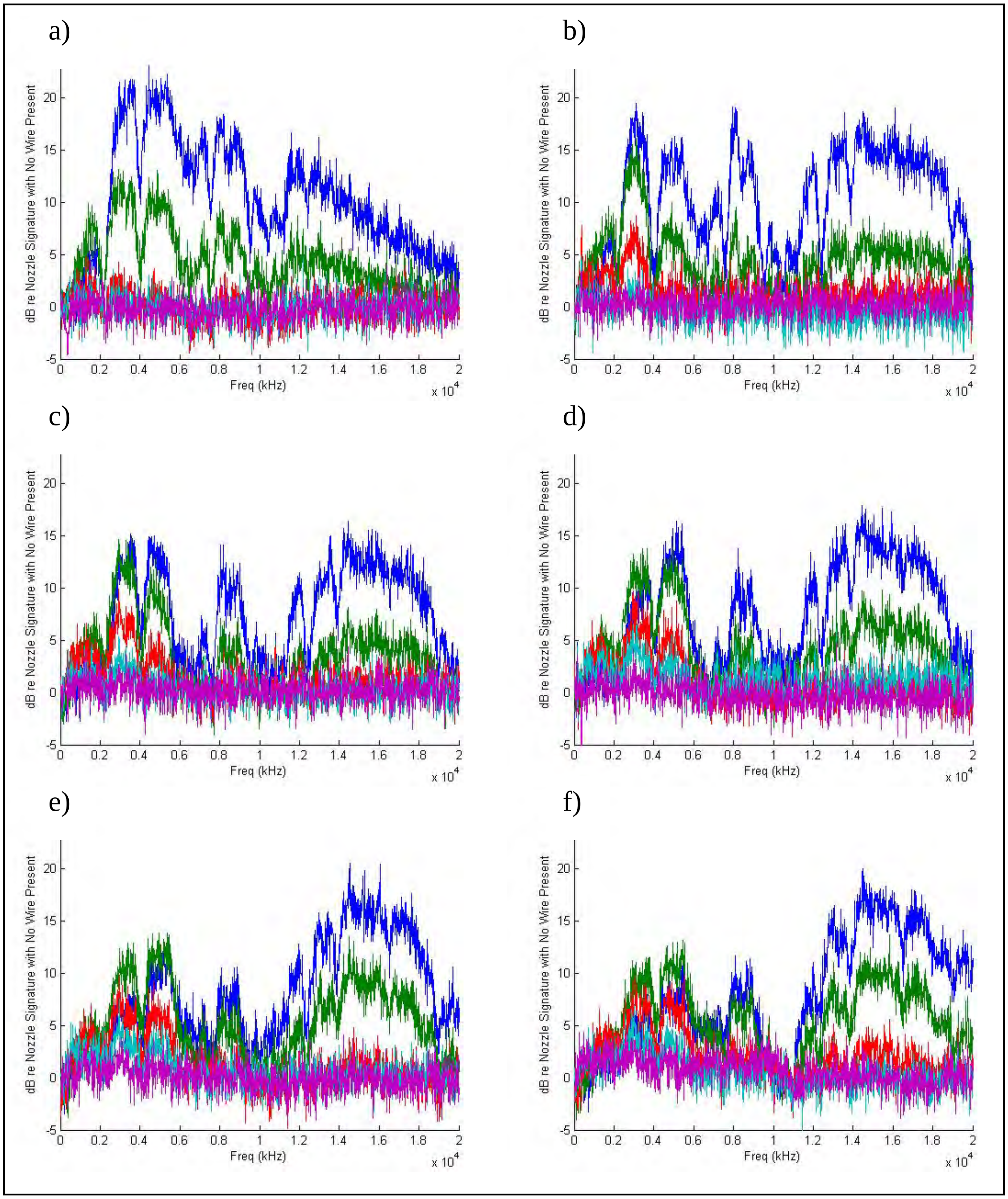

Figure B-10. White cotton string .5 kg tension; single-hole nozzle; microphone at 0° (a) 10 scfh, (b) 20 scfh, (c) 30 scfh, (d) 40 scfh, (e) 50 scfh, and (f) 60 scfh. Color representation as in figure 5.

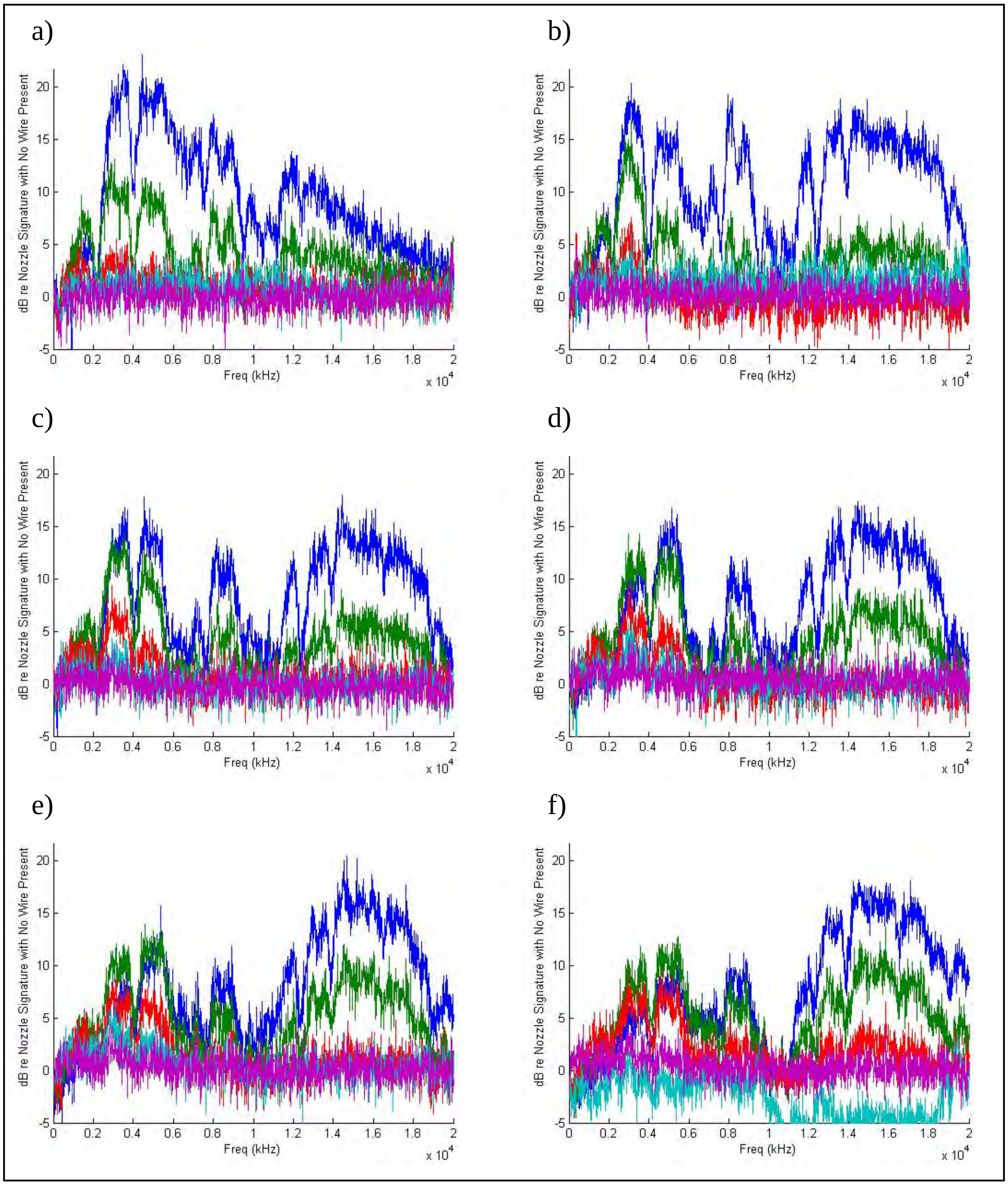

Figure B-11. White cotton string 1.0 kg tension; single-hole nozzle; microphone at 0° (a) 10 scfh, (b) 20 scfh, (c) 30 scfh, (d) 40 scfh, (e) 50 scfh, and (f) 60 scfh. Color representation as in figure 5.

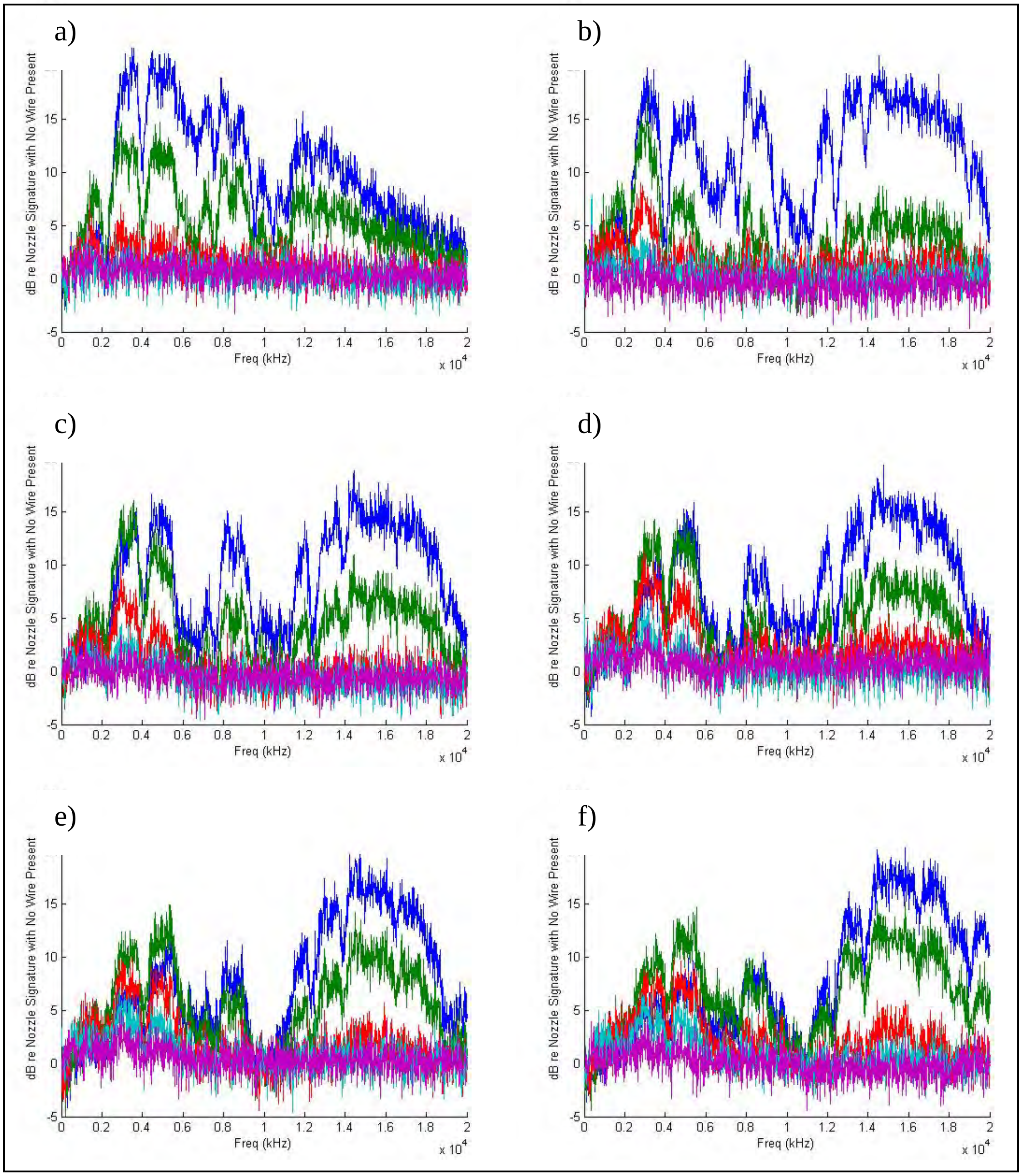

Figure B-12. White cotton string 1.5 kg tension; single-hole nozzle; microphone at 0° (a) 10 scfh, (b) 20 scfh, (c) 30 scfh, (d) 40 scfh, (e) 50 scfh, and (f) 60 scfh. Color representation as in figure 5.

Appendix C. Single-hole Nozzle Non-insulated Mild Steel Wire with Microphone at Different Angles

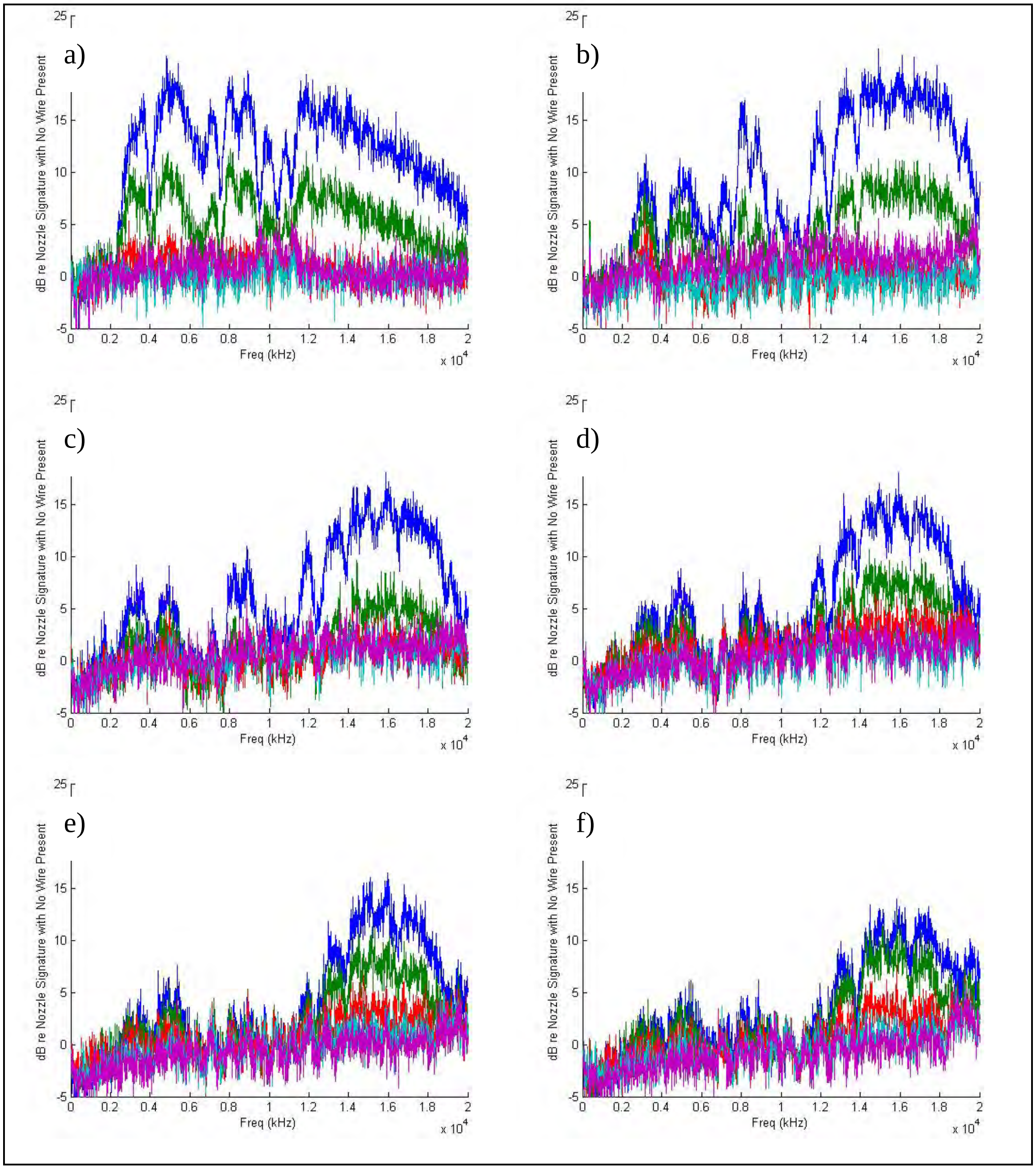

Figure C-1. 0 degrees; single-hole nozzle; non-insulated mild steel wire, zero tension, (a) 10 scfh, (b) 20 scfh, (c) 30 scfh, (d) 40 scfh, (e) 50 scfh, and (f) 60 scfh. Color representation as in figure 5.

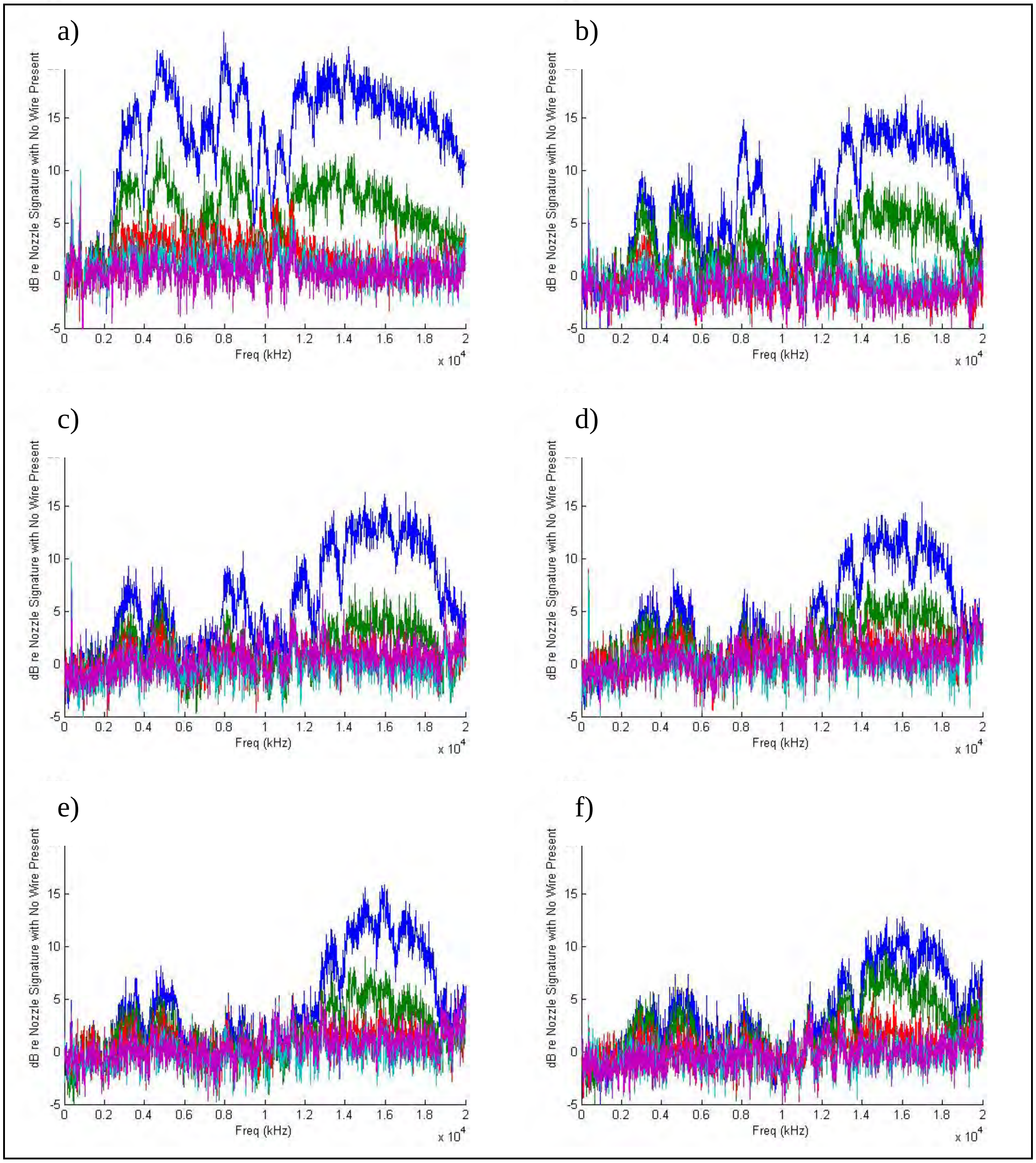

Figure C-2. 45 degrees; single-hole nozzle; non-insulated mild steel wire, zero tension, (a) 10 scfh, (b) 20 scfh, (c) 30 scfh, (d) 40 scfh, (e) 50 scfh, and (f) 60 scfh. Color representation as in figure 5.

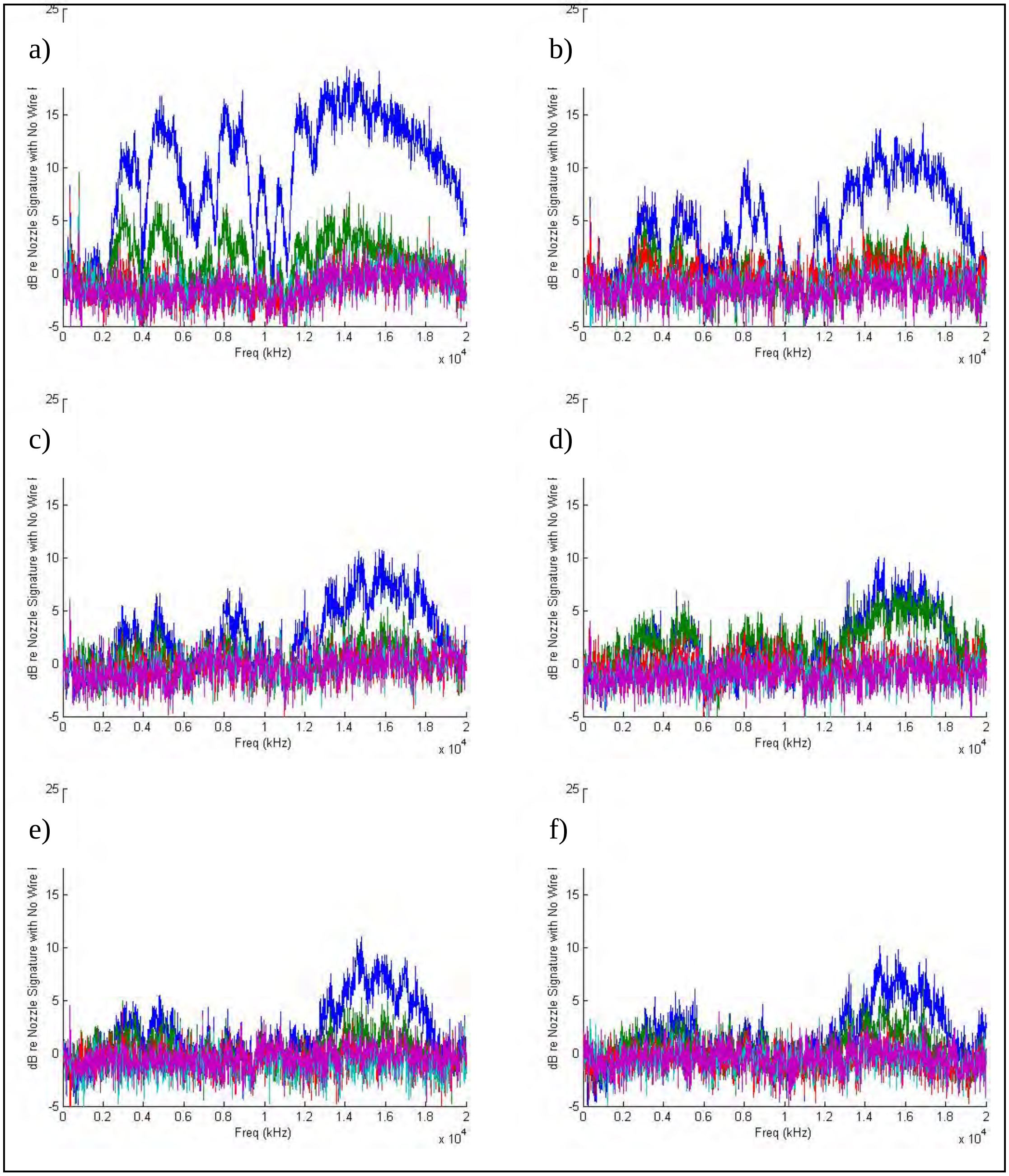

Figure C-3. 90 degrees; single-hole nozzle; non-insulated mild steel wire, zero tension, (a) 10 scfh, (b) 20 scfh, (c) 30 scfh, (d) 40 scfh, (e) 50 scfh, and (f) 60 scfh. Color representation as in figure 5.

NO. OF COPIES	ORGANIZATION
1 ELECT	ADMNSTR DEFNS TECHL INFO CTR ATTN DTIC OCP 8725 JOHN J KINGMAN RD STE 0944 FT BELVOIR VA 22060-6218
1	DARPA ATTN IXO S WELBY 3701 N FAIRFAX DR ARLINGTON VA 22203-1714
1 CD	OFC OF THE SECY OF DEFNS ATTN ODDRE (R&AT) THE PENTAGON WASHINGTON DC 20301-3080
1	US ARMY INFO SYS ENGRG CMND ATTN AMSEL IE TD A RIVERA FT HUACHUCA AZ 85613-5300
1	COMMANDER US ARMY RDECOM ATTN AMSRD AMR W C MCCORKLE 5400 FOWLER RD REDSTONE ARSENAL AL 35898-5000
1	US ARMY RSRCH LAB ATTN RDRL CIM G T LANDFRIED BLDG 4600 ABERDEEN PROVING GROUND MD 21005-5066
1	DIRECTOR US ARMY RSRCH LAB ATTN RDRL ROE V W D BACH PO BOX 12211 RESEARCH TRIANGLE PARK NC 27709
6	US ARMY RSRCH LAB ATTN IMNE ALC HRR MAIL & RECORDS MGMT ATTN RDRL CIE S W ALBERTS II (3 COPIES) ATTN RDRL CIM L TECHL LIB ATTN RDRL CIM P TECHL PUB ADELPHI MD 20783-1197

TOTAL: 13 (11 HCS, 1 CD, 1 ELECT)